VŠB – Technical University of Ostrava

Nanotechnology Centre

University Study Programmes - Nanotechnology

Diploma Thesis

Anchorig of phytosynthesized silver nanoparticles to polycaprolacton fiber matrix for medical application

Kotvení biosyntetizovaných nanočástic stříbra na polykaprolaktonová vlákna pro využití v medicíně

Author Bc. Zuzana Vilamová

Supervisor Ing. Gabriela Kratošová, Ph. D.

Ostrava 2020

VŠB - Technical University of Ostrava
University Study Programmes
CNT - Nanotechnology Centre

Diploma Thesis Assignment

Student: **Bc. Zuzana Vilamová**

Study Programme: N3942 Nanotechnology

Study Branch: 3942T001 Nanotechnology

Title: Anchorig of phytosynthesized silver nanoparticles to polycapronlacton fiber matrix for medical application
Kotvení biosyntetizovaných nanočástic stříbra na polykaprolaktonová vlákna pro využití v medicíně

The thesis language: English

Description:

Polymer-metal based materials with unique 3D structures can find various applications in biomedical field. Diploma thesis is focused on (i) nanosilver colloid and (ii) polycaprolactone (PCL) fibers preparation, characterization of both materials and their mixing to obtain functional product with application potential in medicine. Silver nanoparticles will be prepared by optimized biotechnological protocol using chosen organic acids and anchored on electrospun PCL fibers. PCL fibers will be prepared through electrospinning in cooperation with Technical University in Liberec and electrospraying in cooperation with PrimeCell Advanced Therapy Company. Various analytical and imaging methods will be employed for materials characterization. Functionality of prepared PCL-Ag material will be verified in antimicrobial testing.

The particular aims of thesis are specified as follows:
1) review available literature and summarize current knowledge about the application of nanosilver and PCL in medicine,
2) carry out experiments of PCL electrospinning and silver anchoring on PCL matrix,
3) characterize synthesized nanoparticles and fibers using available imaging and analytical methods,
4) evaluate and discus the best method for Ag nanoparticles anchoring and material usage for medical applications.

References:

NGUYEN, Duong Nhat, Christian CLASEN a Guy VAN DEN MOOTER. Pharmaceutical Applications of Electrospraying. Journal of Pharmaceutical Sciences [online]. 2016, 105(9), 2601-2620 [cit. 2019-10-18]. DOI: 10.1016/j.xphs.2016.04.024. ISSN 00223549. Available from: https://linkinghub.elsevier.com/retrieve/pii/S0022354916413973

KRATOŠOVÁ, Gabriela, Veronika HOLIŠOVÁ, Zuzana KONVIČKOVÁ, et al. From biotechnology principles to functional and low-cost metallic bionanocatalysts. Biotechnology Advances [online]. 2019, 37 (1), 154-176 [cit. 2019-10-17]. DOI: 10.1016/j.biotechadv.2018.11.012. ISSN 07349750. Available from: https://linkinghub.elsevier.com/retrieve/pii/S0734975018301964

STAMM, Manfred. Nanostructured and Nano-size Polymer Materials: How to Generate Them and Do We Need Them?. FAKIROV, Stoyko, ed. Nano-size Polymers [online]. Cham: Springer International Publishing, 2016, 2016-09-02, s. 3-15 [cit. 2019-10-18]. DOI: 10.1007/978-3-319-39715-3_1. ISBN 978-3-

319-39713-9. Available from: http://link.springer.com/10.1007/978-3-319-39715-3_1

LUKÁŠ, D., A. SARKAR, L. MARTINOVÁ, et al. Physical principles of electrospinning (Electrospinning as a nano-scale technology of the twenty-first century). Textile Progress [online]. 2009, 41(2), 59-140 [cit. 2019-10-18]. DOI: 10.1080/00405160902904641. ISSN 0040-5167. Available from: http://www.tandfonline.com/doi/abs/10.1080/00405160902904641

ZHANG, Y. Z., J. VENUGOPAL, Z.-M. HUANG, C. T. LIM a S. RAMAKRISHNA. Characterization of the Surface Biocompatibility of the Electrospun PCL-Collagen Nanofibers Using Fibroblasts. Biomacromolecules [online]. 2005, 6(5), 2583-2589 [cit. 2019-10-18]. DOI: 10.1021/bm050314k. ISSN 1525-7797. Available from: https://pubs.acs.org/doi/10.1021/bm050314k

Extent and terms of a thesis are specified in directions for its elaboration that are opened to the public on the web sites of the faculty.

Supervisor: **Ing. Gabriela Kratošová, Ph.D.**

Consultant: Ing. Zuzana Konvičková

Date of issue: 02.12.2019

Date of submission: 08.05.2020

prof. Ing. Jaromír Pištora, CSc.
Head of Department

Ing. Zdeňka Chmelíková, Ph.D.
Vice-rectress for Study Affairs

AUTHOR DECLARATION

The work submitted in this diploma thesis is the result of my own investigation, except here otherwise stated.

It has not already been accepted for any degree, and is also not being concurrently submitted for any other degree.

……....

Bc. Zuzana Vilamová

DECLARATION

- I was aware of the fact that my diploma work is fully covered by the Act No.121/2000 Coll. Copyright Act, particularly §35 - use of the work within the civil and religious ceremonies, in university performances and school use of the work and §60 – schoolwork.
- I acknowledge that the VŠB-Technical University of Ostrava ("VŠB-TUO") has the unprofitable right to use this diploma thesis (§ 35 paragraph 3).
- I agree that the thesis will be electronically deposited in the Central Library of VŠB-TUO for examination and a copy will be kept by the supervisor of the master thesis. I agree that the information about qualifying work will be published in the information system of VŠB-TUO.
- It was agreed with VŠB-TUO, in case of university interest, I conclude a contract with permission to use the work in accordance with §12 paragraph 4 of the Copyright Act.
- It was agreed that use this work; diploma work or to provide the license to other utilization I can do only with the approval of the VŠB-TUO, which is authorized to demand an adequate fee for the costs, which were expended to the creation of this work incurred by VŠB- TUO (until the actual amount).
- I agree that the submission of my work will be published in accordance with Act No.111/1988 Coll., about universities and the amendment of other Acts (Higher Education Act), regardless of the outcome of its defense.

……..

_____

Student's name

_____

Address

Abstract

This diploma thesis focuses on the mechanisms involved in the formation of silver nanoparticles by biosynthesis. Here, the electro-spraying method was employed with poly(vinyl alcohol), and this was combined with silver nanoparticles on a poly(ε-caprolacton) fibrous material. The theoretical part of the thesis describes the preparation and antibacterial properties of silver nanoparticles and their incorporation in polymeric droplets by electrostatic spraying. These processes were conducted to prove the hypothesis that fibrous materials combined with silver nanoparticles have great possibility for application in medicine and especially in wound dressings. The experimental part then demonstrates how silver nanoparticles are prepared by the chosen organic compound - maleic acid - with concentration gradient. This is followed by the attachment of polymeric droplets, and final mixing of the polymer with nanoparticles on the fibrous matrix by electro-spraying. The analyses used to characterise the prepared silver nanoparticles and fibrous materials include electron microscopy, X-ray diffraction and dynamic light scattering. These confirmed that the silver nanoparticles were successfully synthesised, and they were then subjected to antibacterial and cytotoxicity testing to illustrate their worth in the biomedical field. Finally, the electrostatic spraying of poly(vinyl alcohol) and its mixture with silver nanoparticles for attachment to the prepared poly(ε-caprolacton) fibrous matrix was evaluated. This also proved successful and, most importantly, it produced no cytotoxic effect.

Keywords:

biosynthesis; phytosynthesis; maleic acid; silver nanoparticles; electrospinning; electrospraying; poly(vinyl alcohol); polycaprolacton;

Reference format:

VILAMOVÁ, Zuzana. 2020. *Anchorig of phytosynthesized silver nanoparticles to polycaprolacton fiber matrix for medical application*. Ostrava. 73. Diploma thesis. VŠB-Technical University of Ostrava. Supervisor Ing. Gabriela Kratošová, Ph.D.

Abstrakt

Diplomová práce se věnuje studiu mechanismu tvorby stříbrných nanočástic metodou fytosyntézy a elektrostatickému procesu sprejování polyvinyl alkoholu a jeho směsi s připravenými nanočásticemi na polykaprolaktonová vlákna. Teoretická část je z části věnována přípravě a antibakteriálním vlastnostem nanočástic stříbra a částečně elektrostatickému procesu a jeho využití při přípravě antibakteriálních materiálů s potenciálem v medicíně. Experimentální část je zaměřena na popis a charakterizaci nanočástic stříbra, které jsou připraveny pomocí vybrané organické sloučeniny kyseliny maleinové a jejich ukotvení na polykaprolaktonových vláknech za pomoci elektrostatického sprejování směsi polymerního roztoku polyvinyl alkoholu a připravených nanočástic. Pro charakterizaci nanočástic stříbra a vlákenných materiálů bylo použito několik metod, jako je elektronová mikroskopie, rentgenová difrakce, dynamický rozptyl světla, antibakteriální a cytotoxické testování. Nanočástice stříbra byly úspěšně syntetizovány. Připravené vláknité materiály byly vyhodnoceny jako netoxické vůči testovaným buňkám s možnou následnou aplikací v medicíně.

Klíčová slova:

biosyntéza; fytosyntéza; kyselina maleinová; stříbrné nanočástice; elektrostatické vláknění; elektrostatické sprejování; poly(vinyl alcohol), polykaprolakton;

Vzor citace:

VILAMOVÁ, Zuzana. 2020. *Kotvení biosyntetizovaných nanočástic stříbra na polykaprolaktonová vlákna pro využití v medicíně*. Ostrava. 73. Diplomová práce. VŠB-Technická Univerzita Ostrava. Vedoucí práce Ing. Gabriela Kratošová, Ph.D.

Acknowledgement

First of all, I would like to express my thanks to my supervisor Ing. Gabriela Kratošová, Ph.D. and my consultant Ing. Zuzana Konvičková for their advice and for providing all necessary information and their patience during writing this diploma thesis in very friendly atmosphere.

I would like to thank PrimeCell Biosience a.s. to enable me access and working with 4SPIN® device in their laboratory department. Many thanks to Ing. Petr Mikeš, Ph.D for the opportunity to visit the Technical University of Liberec, where I was allowed to create a polymer matrix by Nanospider^{TM}.

I would like to propose my thanks to people interested in characterization methods in my diploma thesis:

- STEM: Ing. Gabriela Kratošová, Ph.D. and Marie Heliová, Nanotechnology Centre (VŠB - Technical University of Ostrava, Czech Republic)
- DLS and size distribution: Ing. Jiří Bednář, PhD., Nanotechnology Centre (VŠB - Technical University of Ostrava, Czech Republic)
- XRD: doc. RNDr. Edmund Dobročka, CSc., Institute of Electrical Engineering (Slovak Academy of Sciences in Bratislava, Slovak Republic)
- Antibacterial assessment: Mgr. Kateřina Rosenbergová, PhD., Faculty of Veterinary Medicine (University of Veterinary and Pharmaceutical Sciences Brno, Czech Republic)
- Cytotoxicity testing: Mgr. Ludmila Porubová, Public Health institute Ostrava (Czech Republic)
- English proofreading: Raymond J. Marshall

I would like to thank my family members that support me all the time and my classmates for creating memories and experiences during our studies.

Contents

List of abbreviations

DLS = dynamic light scattering

DNA = deoxyribonucleic acid

E. coli = *Escherichia coli*

IUPAC = International Union of Pure and Applied Chemistry

LC = liquid chromatography

MS = mass spectroscopy

MTT = 3-(4,5-dimethylthiazol-2-yl)-2,5-diphenyltetrazoliumbromid

Mw = molecular weight

NP = nanoparticle

NC = negative control

PCL = poly(ε-caprolacton)

PEO = poly(ethylene glycol)

PLA = poly(lactic acid)

PLGA = poly(lactic-co-glycolic acid)

PVA = poly(vinyl alcohol)

PVP = poly(vinyl pyrrolidone)

PC = positive control

S. aureus = *Staphylococcus aureus*

SEM = scanning electron microscopy

STEM = scanning transmission electron microscopy

TEM = transmission electron microscopy

XRD = X-ray diffraction

Introduction

The concept of nanotechnology covers research and technology development on the atomic, molecular and macro-molecular levels. This ensures that the final structures are successfully synthesized in the 1-100 nm size range. Nanotechnology incorporates the sciences of physics, chemistry, engineering and molecular biology, and it can therefore be defined as an interdisciplinary and cross-sectional technology which creates and utilises a variety of structures. These include the nanotechnology developmental devices and systems with the unique chemical, optical, electrical, mechanical and thermal properties in their small and intermediate sizes. An example of the complexity of these combined properties is that increases in the surface area to volume ratio dramatically alter the nanomaterial mechanical, thermal and catalytic properties compared to those in bulk materials [1–3].

The theoretical section of the thesis provides a literature overview. The initial part outlines the issue of silver nanoparticle preparation, and their antibacterial properties because these create the most research interest. Phytosynthesis was chosen for nanoparticle preparation because 'green' environmental science is currently so important. Both the advantages and disadvantages of this method are then discussed. Next part outlines the use of silver nanoparticles as antibacterial agent which could improve wound dressings efficiency and can thus treat the wound prevalence in geriatric care. This attachment could be enhanced by the electro- spraying procedure described in the next part of the theory, and the last part concentrates on the preparation of fibrous materials suitable for use as a matrix for silver nanoparticle attachment.

The experimental part of this thesis is devoted to the actual silver nanoparticle preparation and its incorporation in the poly(vinyl alcohol) electrospun droplets attached to the poly(ε-caprolacton) fibres. The success of these processes is then analysed, and this is followed by the testing of its antibacterial properties and cytotoxicity which are so important in medicine today. All experimental results are then discussed.

Theoretical part

1. The beginning of nanotechnology field

Although nanotechnology has been recognised for many years, scientists had little knowledge of nanometer levels. The first utilised nanosized "material" is known from Lycurgus cups manufactured in the 4th century, where the glass cups containing metal Ag and Au nanoparticles (NPs) changed light spectrum colour from green to red. The coloured glasses in medieval churches and cathedrals are also due to different metal NPs [1].

After many centuries, the first pioneer in nanotechnology was Richard Feynman, an American physicist, scientist and Nobel Prize laureate in physics who is famous for his contribution to quantum electrodynamics. His lecture called "There's plenty of room at the bottom" given at the American Physical Society meeting at the California Institute of Technology introduced the possibilities of manipulating tiny objects to generate specialised materials. This process is now advanced by scanning tunnelling microscopy [4]. He also predicted the invention of electron beam lithography [5], which is currently used for silicon chip production in the electronic industry [6].

More recently, ferrofluids, particles produced by milling and colloids were among the substances used in the 1960's for preparation of new materials with unique properties, and this was followed by inventions of the scanning tunnelling microscope and atomic force microscopy in the 1980's [1].

A new interdisciplinary field of nanotechnology has now been created by increased scientific interest in new nanomaterials and material preparation and characterisation by instruments such as the scanning and transmission electron microscope (SEM, TEM) [1, 6]. The special structural properties at the nanometre level can be used in many areas such as material engineering. Examples of this include increasing material photocatalytic activity [7], detecting ions in the chemical industry [8] and adsorption of CO_2 [9]. Nanotechnology is now very promising in biomaterial research and most important in medicine and pharmacy applications [10, 11].

2. Preparation of metal and metal-based nanostructures

The “Bottom-up” and “top-down” methods are basic approaches to obtain nanostructured materials. Examples of the "top-down" method are ball-milling and laser ablation, and these methods start with bulk material and lead to their reduction to micro- and nano-scale size. In contrast, the "bottom-up" process builds structures from elementary building blocks such as atoms and molecular constituents into an organised structure, and this approach is used in chemical reduction, precipitation and organic synthesis [12, 13].

Nanostructured material preparation, including particles, films and fibres can be divided into four main categories: (1) physical, (2) chemical, (3) mechanical and (4) the biotechnological approach shown in Figure 1 [12, 13].

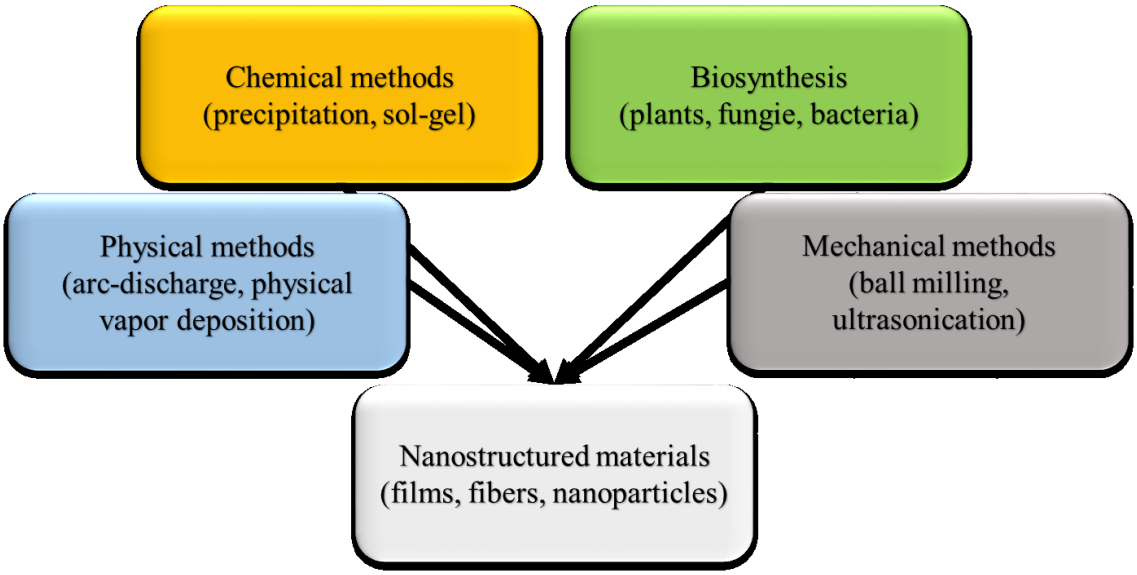

Figure 1: Diagram of four ways of preparing nanostructured materials. The many ways currently in use range from sol/gel methods to ball milling and biosynthesis.

2.1. Physical and mechanical approaches

Physical “top-down” methods include arc-discharge in liquids, and sputtering is a physical approach used in “bottom-up” procedures. Sputtering is most beneficial when single atoms or molecules are processed in controlled conditions, such as heating, to create substances without the undesired side-effects of dislocation and precipitation [12] An appropriate example of sputtering is its use in creating a thin layer of TiO_2 for solar panels [14].

However, one disadvantage of using physical methods is the necessity of stabilisers to prevent aggregation of NPs which may be toxic and harmful. Physical methods can also be economically and energetically demanding, especially when they require expensive equipment such as lasers and specialised conditions of high or low pressure or temperature. In contrast ,one advantage of this physical methodology is the narrow range of resultant NP size distribution [12].

Typical examples of mechanical methods are ball milling [14] and reactive milling [15]. Although these processes are simple, rapid and economically undemanding, they cannot be used in industry because of their wide range of NPs size distribution and low purity. Milling, however, can be beneficial when large amounts of metallic and ceramic NPs powders, amorphous alloys and nanocomposites are required [12, 13].

2.2. Chemical and biotechnological approaches

Although many "bottom-up" approaches have been developed, their use for chemical methods have the disadvantage of expense and possible toxicity. The final NPs, however, are often homogenous in size distribution, with high probability of repeatable results and the final NPs shape is easily designed and controlled. A novel chemical method involves the use of organic molecules, such a usnic acid, thymol [13] and other molecules [8, 16]. These naturally occurring organic molecules are closely related to biosynthesis [1] and they are of major importance. The main principles involved in pure natural organic acids and flavonoids are discussed in chapter 3.3.

Natural biomasses are able to reduce metallic NPs by mixing with an initial metal salt precursor. These biomasses include phytosynthetic vascular plants and their leachates and extracts [17], microscopic mycosynthetic fungi [18] and algae [19]. It is mainly the organic compounds from the biomass which are used in synthesis, and this process can also be considered a chemical method. The main advantages of this biotechnological method is that NP synthesis and stabilisation occur in one step and it can be mediated by organic compounds of biomass origin under the following conditions:

(1) reduction or elimination of chemical solvents and toxic reagents

(2) minimised energy consumption and the use of mild experimental conditions,

(3) less waste, and

(4) increased safety.

Biosynthesis is an environmentally friendly process which avoids the presence of hazardous and toxic solvents and waste and it is economically advantageous for NPs production without the need for special equipment or devices. Therefore, biosynthesis can be considered a “green chemistry” method. Limitations, however, include difficulty in describing biosynthesis mechanisms and possible biomass contamination [12, 20]. This is further discussed in chapter 3.2.

3. Metal and metal-based nanoparticles use in medicine

NPs are defined by their three dimensions at 100 nm or less, and their most common form is solid and colloidal particles. The advantages over larger particles include increased surface to volume ratio, higher antimicrobial activity and improved magnetic properties [21]. One example is Fe_3O_4/Fe_2O_3 iron oxide NPs which are used as magnetic resonance spectroscopy contrast agents for biological and cell imaging and in thermal therapeutic applications. There are then also the Au, TiO_2, ZnO, Cu- and Ni- based NPs with reported antimicrobial activity and drug delivery benefits [21].

This thesis focuses on describing the processes involved in the preparation, properties and medical applications of nano-silver. Ag NPs have great potential in medicine as antimicrobial agents [17, 22], diagnostic and optoelectronic platforms [23]. Figure 2 highlights the Ag NPs sizes and rod-like, triangular and circular shapes referred to in studies on its ability to alter its final properties These characteristics can be manipulated during synthesis by the choice of reducing agent, stabiliser, pH and temperature[24].

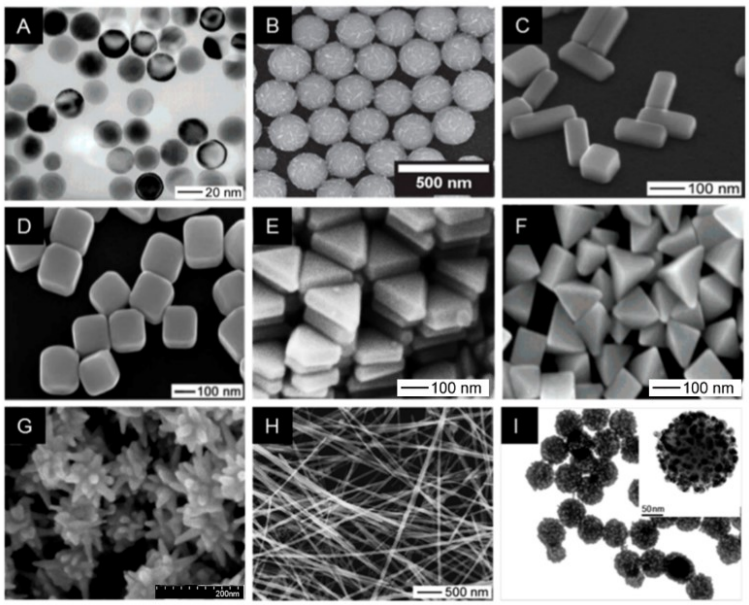

Figure 2: SEM and TEM images of diverse Ag nanostructure shapes and sizes; (A) nanospheres, (B) necklaces, (C) nanobars, (D) nanocubes, (E) nanoprisms, (F) pyramides, (G) nanostars, (H) wires and (I) spherical NPs loaded by silica NPs [24].

The choice of Ag NPs, for both this article and its filler-role in wound dressings, was inspired by their antimicrobial activity and proven Ag^+ ion release. Ag NPs in aqueous

environments oxidise and release ions because of proton and oxygen presence. The Ag^+ ions release-rate depends of factors including their size, shape and the colloid capping agent [24-26]. However, Ag NPs cytotoxicity effects are similar for both bacteria and humans, and therefore enhanced antimicrobial treatment in clinical medicine can be induced by altering a larger surface area of Ag NP properties. These include morphology and size changes to provide a larger surface area, use of a higher concentration and a more rapid Ag^+ ion release rate. Ag^+ ion and Ag NP cell damage can be characterised by four main Ag NP principles:

(1) Ag NPs aggregate and adsorb to the cell surface, thus damaging its membrane and transport ability;

(2) Ag NPs and ions penetrate and interact with cellular organelles and biomolecules which affect cellular functions including permeability and respiration;

(3) Ag NPs and ions inside the cell can help generate reactive oxygen species and subsequent cell damage; and

(4) NPs can interact with the bacterial deoxyribonucleic acid (DNA) and cause loss of transcription and replication.

The Ag NPs and/or Ag^+ ion penetration mechanism and cell destruction are briefly indicated in Figure 3.

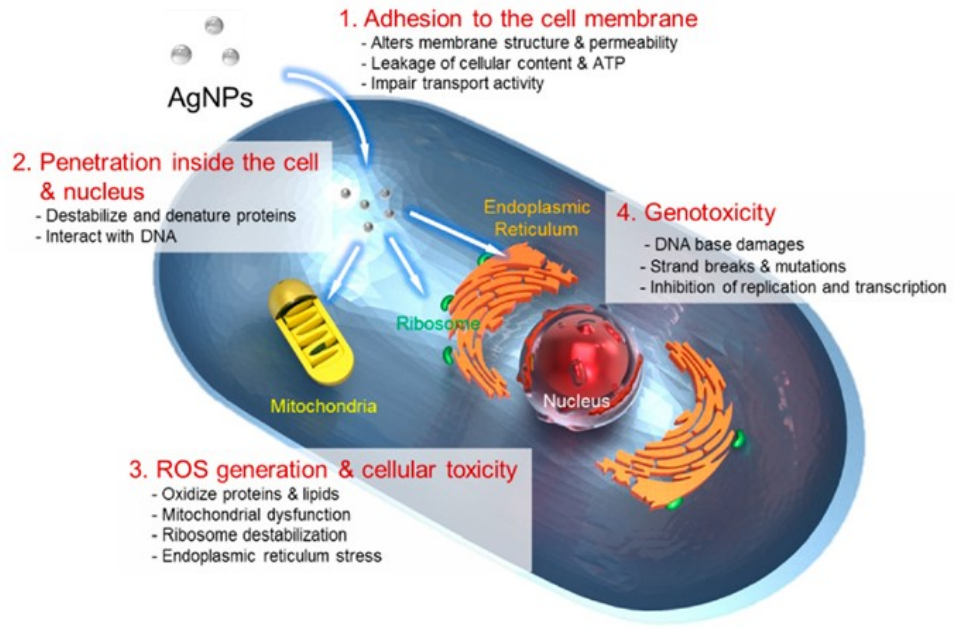

Figure 3: Ag NPs' main cell destruction mechanisms [24].

Chemical reduction in the noble metal precursor liquid is one of the most popular methods of producing Ag NPs. Examples here include silver nitrate ($AgNO_3$), acetate (AgC_2H_3O) and sulphate (Ag_2SO_4) use with an appropriate reducing agent [24, 26]. Ag NP nucleation and growth mechanisms in colloidal solution are now discussed.

3.1. Silver nanoparticles nucleation and growth in liquid medium

The chemical and biotechnology "bottom-up" approach enables $AgNO_3$ salt precursor metal ions to be transformed to zero-valent form when the reducing agent and precursor are mixed (Figure 4) [24].

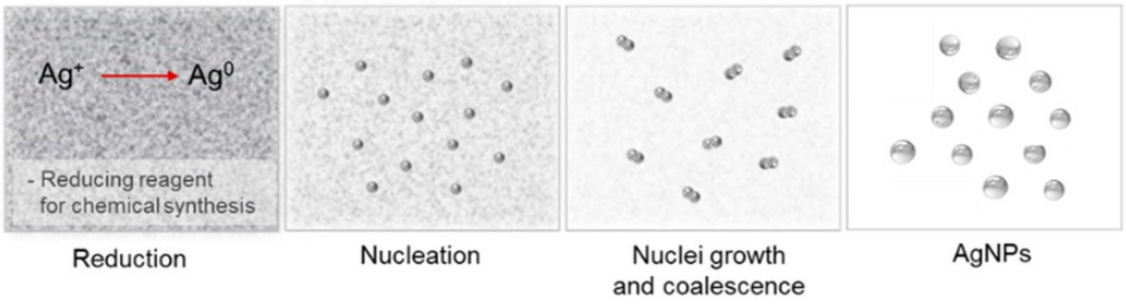

Figure 4: Synthesis of Ag NPs, their nucleaction and growth in colloid using the bottom-up chemical and/or biotechnology method [24].

Figure 5 shows the La Mer model and its modifications most commonly used to describe the NPs' nucleation and growth mechanisms. The NP nuclei are created homogenously in the entire colloid volume, and its stabilisation by organic compounds occurs simultaneously. The precursor concentration increases after mixing, and this first stage creates (1) a degree of saturation. Nucleation then occurs in the second stage (2) with a large number of nuclei created when the level of saturation surpasses the critical nucleation threshold. Finally, the third phase is nanoparticle growth which proceeds as follows:

(3) monomer addition/diffusion growth occurs and additional precursor units deposit on the nuclei surface;
(4) Ostwald ripening ensures that energetically disfavoured small nuclei are re-dissolved and deposit on more thermodynamically stable larger nuclei; and
(5) coalescence and aggregation occurs, where several NPs join together [12, 26, 27].

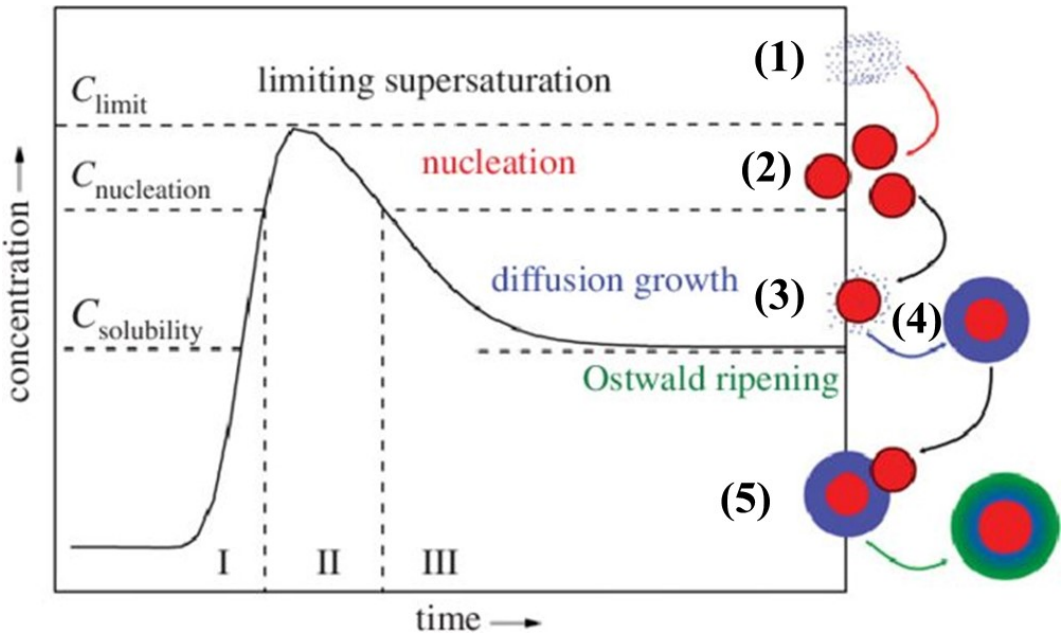

Figure 5: The principle of NP nucleation and growth due to LaMer mechanism for mono-dispersed colloids; I – precursor monomers, II - nucleation, III – NPs growth [27].

However, the LaMer model and its modification cannot predict size distribution evolution or final NP morphology. It is most important to know these parameters because they have major effects on antibacterial ability and toxicity [12, 27]. The NPs size, shape, crystallinity and aggregation ability are all influenced by temperature, pH and the precursor and reducing agent concentrations, so these must be optimised for particular Ag NPs synthesis and their intended application [24, 26].

Ag NPs can therefore be prepared with controlled size and specialised shape. These include the nanowires and nano-cubes which can be produced in multivalent alcohol 'polyol' synthesis with polyethylene glycol as the reducing agent. The polyvinylpyrrolidone (PVP), poly(vinyl) alcohol (PVA) or polyethylene glycol [28] polymer stabilisers in this synthesis [29] must be present to prevent NP agglomeration [26]. Ag NPs preparation by 'green' phytosynthesis is now described.

3.2. Resolving phytosynthesis mechanisms

This thesis on Ag phytosynthesis has a biotechnological approach, and it stresses that phytosynthesis is based on plant exploitation [8]. This especially focuses on leachates [3] and extracts [10], but it also includes the fruit and leaves [9]. All these constituents contain the phytochemical biomolecules directly involved in reduction, formation and stabilisation

of metallic NPs in solution. The biosynthesised NP size, shape and concentration are directly influenced by phytosynthetic parameters of temperature, pH, precursor concentration, biomass quality, biomass/precursor ratio, exposure time and solution mixing. Controlling these parameters enables optimised NPs' characteristics and size [3, 11].

There is inherent difficulty in describing the general biosynthesis mechanisms and NP stabilisation processes because each biomass is a unique complex system of many organic biomolecules. These include quercetin [29, 30], kaempferol [29], protacatechuic acid [30] and rutin [30], all with their individual positively and negatively charged functional groups. Examples of negatively charged groups include -OH hydroxyls, $-NH_2$ aminos and the -COOH carboxyl groups [17].

Experimental difficulties arise in the repeatability of biosynthesis experiments and control of the prepared NPs' morphology and crystallinity. While these require further optimisation, they constitute typical issues which can be intuitively solved when working with biological materials. Further possible phytosynthesis problems are created within the used biomass because individual plants and their blossom and leaf components can contain different phytochemical content or contamination. Monitoring natural or anthropogenic contaminants from chemical elements such as Cl^-, Na^+ and NO_3^- in the original biomass is also essential. Thankfully, however, bio-inspired synthetic protocols have shown promise in minimising environmental impacts, and correct biomass combinations have been experimentally optimised to obtain functional NPs with the desired properties [12, 17, 20, 26].

As previously stated, the resolution of phytosynthesis mechanisms is complicated by the complex spectrum of organic compounds in the biomass. However, it is suggested in this thesis that the biosynthesis mechanism can be investigated by two pathways;

(1) testing many different extracts and leachates with similar organic compounds to discover the mechanism or

(2) employing known phytochemicals in the biomass as standards to establish the role of individual bio-compounds as a reducing agent, a stabiliser or both [12].

Alkaloids, terpenoids [12] and flavonoids [30] are organic compounds present in the biomass and these act as reducing agents. Analytic methods such as liquid chromatography (LC) and mass spectrometry (MS) then enable identification of individual

phytochemicals present in the biomass and possible elucidation of the biosynthesis mechanism [12].

LC first separates the compounds in a complex liquid mixture, such as plant extract or leachate, based on their different polarity in the sample and their interaction with the column. Each component in the sample interacts slightly differently, and this separates the components as they flow through the column. At the end of the analysis, these compounds in the liquid sample can then be identified by MS and quantified [29, 30].

An example of leachate composition was supplied by E. Aguirre-Hernández et al [29]. These authors used LC to confirm the presence of flavonoids such as quercetin and kaempferol in leachate. A further study by A. Oniszczuk and R. Podgórski [30] later proved the presence of organic compounds including quercetin, rutin and astralgin.

It is most important that monitoring reactions between precursors and individual phytochemical standards can help predict which plant groups have the potential to produce NPs. However, each phytosynthesis mechanism is specific and complex, and the NP phytosynthesised product is dependent on the original mixture of all contained phytochemicals. These unique properties make each phytosynthesis inimitable [12, 26].

3.3. Silver nanoparticles synthesis by organic compound standards

I have taken a second pathway in this thesis to uncover NP synthesis mechanisms. Herein, I examined Ag NPs synthesis by known organic compounds present in plant leachates. The following overview of this mode of synthesis links biosynthesis with the chemical approach.

Jain and Mehata [31] synthesised Ag NPs using reducing and stabilising agents contained in the *Ocimum sanctum* leaf leachate and also the standard chemical quercetin flavonoid present in the leachate ($C_{15}H_{10}O_7$). $AgNO_3$ was used as precursor, and the resultant Ag NPs had similar characteristics. They both had spherical shape, the similar size distribution in the 10–40 nm range featured in Figure 6 and antibacterial activity against *Escherichia coli* (*E. coli*). The authors demonstrated that the quercetin present in the leachate was mainly responsible for the resultant Ag NP reduction [31].

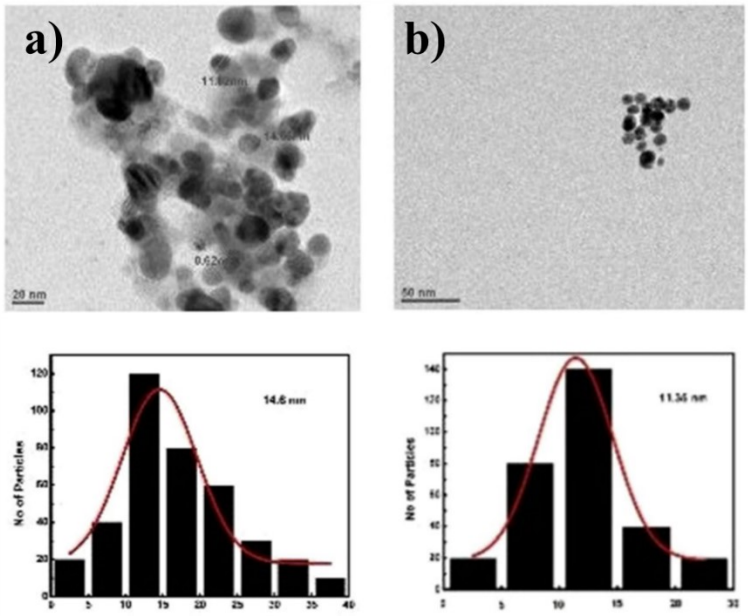

Figure 6: TEM images of AgNPs from (a) leaf leachete Ocimum sanctum; scale bar 20 nm, and b) flavonoid quercetin; scale bar 50 nm, and their size distribution [31].

The NPs produced by quercetin had a higher degree of stability than those prepared by the leachate. They then increased the stability of Ag NPs by increasing colloid pH to 10 with NaOH [31]. The possible mechanism involved in reducing Ag NPs by the quercetin present in the *O. sanctum* leachate can be described by the chemical bonding changes in Figure 7.

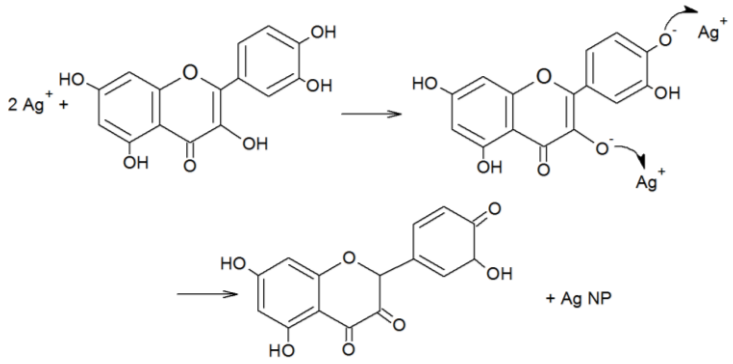

Figure 7: Reduction mechanism of the Ag^{+}ion to Ag NPs by quercetin molecules present in O. sanctum liquid extract [31].

The authors considered that the -OH functional group present in quercetin molecular structure participates as the reducing agent, and that the $AgNO_3$ metal precursor dissociates

in water to Ag^+ and NO_3^- ions. The most reactive quercetin -OH functional group attached to the aromatic carbon ring reacts as an acid with the Ag^+ ion, and this produces the Ag^+ ions reduction to Ag NPs and consequent stabilisation [31].

Alavi and Naser then utilised the *Artemisia haussknechtii* plant [22] and the *Protoparmeliopsis muralis* lichen [32] to synthesise a wide range of NPs. These included Ag, Cu, TiO_2, ZnO and Fe_3O_4 NPs. The authors then used insights gained in those experiments in their recent 2019 study [13]. This focused on describing the biosynthesis mechanism using the usnic acid and thymol present in high amounts in the previously tested plants. Although the chosen compounds proved antibacterial activities, the major antibacterial activity from Ag and Cu metal NP synthesis came from the metal NPs.

The researchers considered that the likely mechanism of metal NPs reduction featured in Figure 8 herein constituted a tautomeric transformation of thymol and usnic acid -OH groups from the enol to keto form. The reactive hydrogen atom released during this transformation reduced the metal ion in the salt precursor to NPs [13]. While this exact mechanism was previously reported by Jain and Mehata [31]. Both studies described only the nucleation and growth of zero-valent Ag NPs [13, 31].

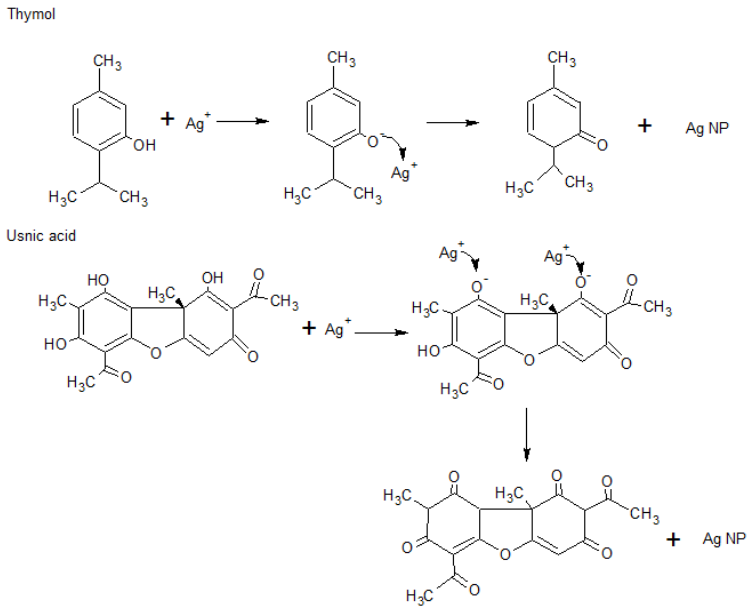

Figure 8: The likely mechanism of metal NPs reduction by thymol and usnic acid described by A.Mehran and K. Naser [13].

Sahu et al. [16] successfully synthesised Ag NPs using the hesperidin, naringin and diosmin flavonoids as secondary citrus plant metabolites and then studied the possible biosynthesis mechanism. They confirmed that the individual -OH groups of flavonoids caused Ag^+ ion reduction to Ag NPs. They reported increased Ag NP stability and better bacterial and cytotoxic properties when naringin was used as the reducing agent in preference to the other two flavonoids [16]. Table 1 shows Ag NP properties prepared by different organic phyto-chemicals.

Table 1: Examples of Ag NP properties prepared by different phyto-chemical compounds.

Organic compound	Diameter [nm]	Shape	Reference
Quercetin	10-40	Spherical	[31]
Thymol	40-120	Spherical	[13]
Usnic acid	18-25	Spherical	[13]
Hesperidin	5-50	Oval	[16]
Naringin	5-40	Oval, spherical	
Diosmin	20-80	Triangular, hexagonal	
Gallic acid	5-20	Spherical	[8]
	4-12	Spherical	[33]
	10-20	Spherical	[25]

4. Electrohydrodynamic process as an efficient tool for preparation of nanostructured materials

Electrostatic effects on liquid droplet generation were first noted in the 17th century and electrostatic spinning methods were improved by J. F. Cooley and W. J. Morton at the beginning of the 20th century [34]. Classic needle electro-spraying and electrospinning procedures were then designed by J. Zeleny [35]. Unfortunately, transmission and scanning electron microscopy technology was not available, and scientists could not detect nano-fibre presence. However, fibre industrial potential was finally recognised in the 1980's and electrospinning has now been intensively investigated for the past 20 years [36].

The Nanospider and 4SPIN devices are used in the experimental part of this thesis for electro-spraying and electrospinning, and their basic equipment and differences are now discussed; together with the polymer characteristics suitable for preparation of the fibres important in medical applications. Use of these devices has the following advantages:

(1) spinning a wide range of polymers,
(2) the variability of parameters that can be applied in the processes, and
(3) easy maintenance of the devices and their components.

Czech scientist Professor Oldřich Jirsák from the Technical University of Liberec and the Czech Company Elmarco developed, constructed and patented the unique Nanospider™ needle-free device. This cylindrical spinning electrode has changed to metal wire, but the same procedure of covering by polymeric solution and high voltage use for fibre generation still applies. The apparatus is easy to operate, and fibrous samples can be produced for commercial use because the final web is larger than 1m [36, 37].

The CONTIPRO Czech company then contributed to nanotechnology in the 1990's by developing the 4SPIN® needle device. Its main advantage over the Nanospider™ is its ability to produce an ordered fibre structure using a rotating collector. This 4SPIN® technology has therefore proven best for rapid laboratory preparation of various materials

4.1. Basic arrangement of the simple device used for droplet and fibre generation

Both electrospinning and electro-spraying processes require a simple device easily installed in a standard laboratory using specific safety precautions. The device has the following three main components (Figure 9):

(1) a solution container, such as a syringe, connected to a pumping system;

(2) a grounded static or rotating collector and

(3) high voltage supply.

The regulation of ambient conditions such as temperature, humidity and other parameters required to control the drying process and non-contamination of final samples necessitates isolation in a closed laboratory chamber [38–40].

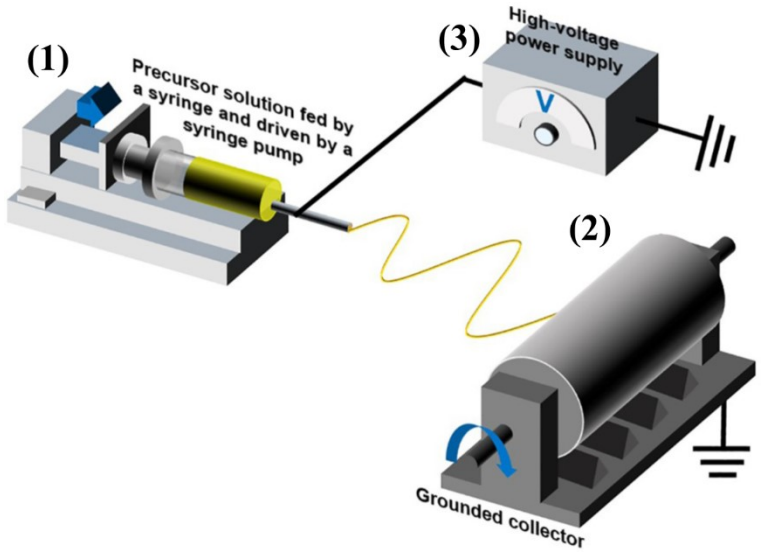

Figure 9: Schematic set-up for preparing nanodroplets/fibres by the electrostatic process. The typical electrospraying/electrospinning device comprises a syringe connected to a pumping system, collector and high voltage supply [38].

The high voltage supply creates an electrostatic field that forms an electric current in the conducting solution ejected from the syringe by the pump. As the intensity of the electric field increases, the spherical shape of the liquid at the tip of the capillary becomes longer and this results in creation of a conical shape called the Taylor cone-jet. The extracted droplets or fibres travel to the collector and the solvent evaporates [38–40]. The following main parameters influence this process;

(1) technical parameters include the type of syringe, the applied voltage and flow rate;
(2) solution parameters are viscosity, conductivity, molecular weight (Mw) and the type of polymer used; and
(3) environmental parameters include humidity and temperature [36, 38–40].

The final properties of the micro-nano-scale droplet or fibre are easily influenced by simple manipulation of the configured arrangements. These include using single, coaxial or tri-capillary needles. The rotating or static collectors can then alter fibre orientation from a non-uniform pattern to a specified direction and care must be taken in increasing applied voltage because extremes can cause defects such as droplets and beads on fibrous samples [36, 38–40].

Electrohydrodynamic processes can also be used to prepare ceramics [44], polymers [3] and others nanostructured objects such as fibres [45] and droplets and particles [46]. Polymers, however, are the most frequently used materials for electrospinning and electro-spraying. High Mw polymers can form fibres, but decreased jet-stream tension created by low Mw polymers forms droplets. Finally, the solution surface tension and viscosity can be reduced by using different solvents, such as ethanol [36, 38–40].

The appropriate 3D structural arrangement for medical application mimics the natural extracellular matrix required for cell attachment and growth. These 3D structures can comprise degradable or non-degradable biomaterials depending on required application, and synthetic materials such as PVA or poly(ε-caprolacton) (PCL) and natural materials including chitosan and collagen can be used for creating the 3D structures. Although natural materials enable impulse transfer between implemented cells and surrounding patient tissue, the synthetics produce better mechanical and chemical stability in the resultant 3D structure [41].

4.2. Electro-spraying for biomedical applications

The main advantages of using electro-spraying in medicine are the production of bioactive agents such as NPs [42] and droplets which act as carriers for drug delivery [38, 39, 43]. This is discussed in greater detail in a later chapter.

The main advantage of using electro-spraying in medical field is fabricating droplets as carriers for drug delivery system [42] or bioactive agents such as NPs, which were discuss detailed later [38, 39, 43].

Electrospraying is often employed because it provide:

(1) improved solubility of poorly water-soluble materials when dispersed in tiny droplets;

(2) bio-electro-spraying provides cell suspensions or encapsulated cells in bio-polymers. These can be sprayed under small applied voltage to avoid cell destruction [43]; and

(3) pharmaceutical, peptide and enzyme delivery in controlled release.

Figure 10 highlights the two main electro-spraying processes by single and coaxial needle [38, 43].

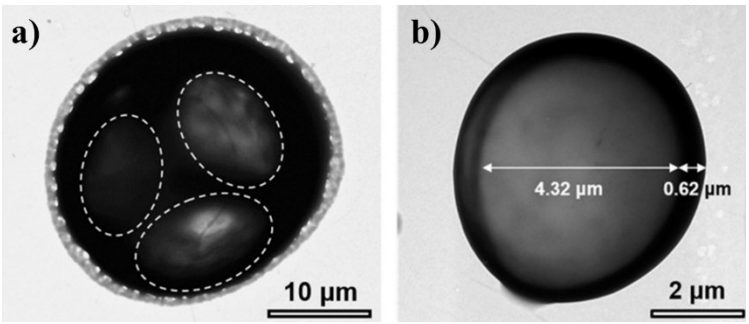

Figure 10: TEM images of differences in internal PLGA droplet structures prepared by; a) single and b) coaxial needle [38].

Figure 10 a) above reflects the following possibility of production of the drug delivery system where bioactive agent such as Ag NP [44, 45] or antibiotics such as silver sulfadiazine [45] or chlorhexidine [44] in a single polymer solution are present [44, 45]. Bioactive agents can be (1) encapsulated in a volume of droplets, or (2) an agent which can be adsorbed to the polymer droplet surface by weak interactions from hydrogen bonding or electrostatic forces. Unfortunately, the adsorption mechanism has disadvantages caused by small amounts of active agent or inappropriate and rapid desorption of the active agents [38, 43].

Encapsulation is often reported in scientific publications, and the ensuing droplet preparation is simple and can be maintained in the following ways: (1) the bio-agents are homogenously dissolved in polymer solution by stirring or ultrasonication and then easily electro-sprayed or (2) bio-agents interact with the droplets in the particle collection bath giving cross-linking and new bond formation, and the droplets can then be collected.

Both methods ensure high encapsulation efficiency and a large amount of primed drug molecules; even up to 100 % [38, 43].

Phenolic acids and flavonoids constitute a wide group of bioactive compounds with potential application in both medicine and the food industry, and their encapsulation in droplets is now assessed. Phenolic acids have poor stability and solubility, and encapsulation by electro-spraying therefore appears promising. The release of active compounds can be controlled by use of an appropriate polymer solution [46]. PVA was the chosen Ag NP carrier in this diploma thesis because of its low toxicity and biocompatibility.

Figure 10 b shows the core-shell structures prepared by the coaxial electro-spraying process, and these are assessed for appropriate use in medicine. The preparation of these structures must be skilled because two immiscible liquid solutions are required. The bioactive agents can be present in the droplet core covered by the protecting shell or they can be encapsulated by another polymer. This is important in the production and further application of hydrophilic-and-phobic droplets [38]. For example, Zamani et al. [47] prepared and investigated core-shell droplets where the core was filled with the bovine serum albumin protein and the shell comprised poly(lactic-co-glycolic acid) (PLGA) for pharmaceutical delivery.

4.2.1. Poly(vinyl) alcohol use in electro-sprayed encapsulation

PVA is a crystalline water-soluble polymer without characteristic odour. It is slightly soluble in ethanol, and Figure 11 highlights that the polymer is composed of repeated units of vinyl-alcohol monomers. PVA has been recognised for many years since it was first prepared in 1924 by Hermann and Haehnel's hydrolysis of polyvinyl acetate. PVA is a widely used synthetic polymer in many medical applications because it has high biocompatibility, low toxicity and low tendency for protein adhesion. PVA is resistant to oils of animal, vegetable or mineral origin and also organic solvents such as aromatic and aliphatic hydrocarbons, esters, ethers and ketones. It is ductile, strong but flexible [48].

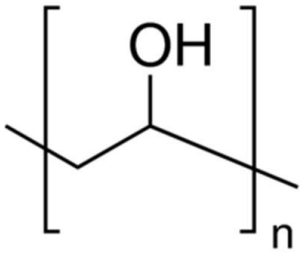

Figure 11: Repeating PVA unit recorded in the International Union of Pure and Applied Chemistry (IUPAC).

PVA solubility depends on its Mw and degree of hydrolysis. Its physical properties depend on the degree of polymerisation, hydrolysis and the Mw which generally varies from 9,000 to 180,000 $g \cdot mol^{-1}$. These properties also affect PVA solubility in water, and it is currently accepted that PVA can be hydrolytically biodegraded by fungal origin present in water ecosystem [48]. The mechanical strength increases with increasing polymerisation, and high air humidity induces increased PVA film and fibre softness and flexibility. It is therefore essential to determine the optimal combination of those properties to produce the most suitable mechanical properties for application. The final PVA properties can also be affected by mixing with other polymers or fillers in the polymer solution whenever practical [48].

4.3. Materials for fibre production via electrospinning

Nano-fibres with nanometre diameters in units-to-hundreds have become significant over the past 20 years [3]. Water insoluble synthetic polymers such as polyacrylonitrile, polyvinylidene fluoride, and polyurethane and water-soluble synthetic polymers including PVA, PVP, and polyethylene glycol (PEO) can be spun into nano-fibres. These materials are then used as carriers for bioactive agents, such as NPs [17], or used as templates or artificial fibres to form fibrous products with complex and unique 3D structure. The biodegradable synthetic polymers, PCL, polyglycolic acid, polylacid (PLA) and their copolymers such as PLGA have many advantages for wide use in electrospinning [38].

The water-insoluble PCL polymer was chosen as the fibre matrix in this diploma thesis because its hydrophobicity is most important for wound dressing application in medicine. Incidentally, its fibres are stronger than PVA fibres.

4.3.1. Polycaprolacton use as a fibrous matrix

Figure 12 shows that the synthetic PCL polymer has hexanoate repeating units of aliphatic polyester (1,7)-polyoxepan-2-one. PCL was first described by Van Natta et al. [49]. It is hydrophobic, semi-crystalline, soluble at room temperature and has low 59–64 ºC melting point and approximately -60 °C glass transition temperature [50, 51].

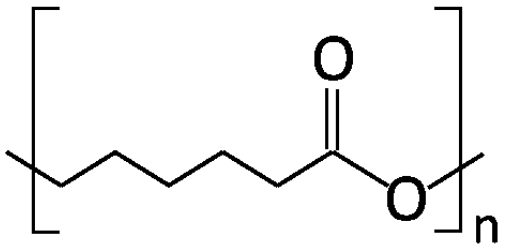

Figure 12: The repeating unit of (1,7)-polyoxepan-2-one recorded IUPAC.

PCL dissolution at room temperature is aided by chloroform, dichloromethane, benzene and toluene. While acetone, dimethylformamide and acetonitrile dissolve PCL to a limited extent, it is insoluble in alcohol, petroleum ether, diethyl ether and water [51].

PCL is assessed in this thesis because of its ability to degrade in human physiological conditions. It is also widely investigated for its physical, thermal and mechanical properties which mainly depend on it 3,000-80,000 $g \cdot mol^{-1}$ Mw and degree of crystallinity. PCL can be mixed with a wide range of polymers for the formation of copolymers such as PCL/PLA and PCL/cellulose [50, 51].

PCL is degraded by ester linkage hydrolysis under human physiological conditions and this is induced with both the following mechanisms occurring simultaneously:

(1) non-enzymatic hydrolytic cleavage of ester groups, and
(2) intracellular degradation by enzymes with high crystallinity and less than 3,000 $g \cdot mol^{-1}$ Mw.

These steps are investigated herein because of PCL's importance as a matrix for long-term pharmaceutical release in humans. [50, 51].

PCL degradation time depends on its morphology, Mw and degree of crystallinity. This ranges from two to four years depending on polymer Mw, and hydrolysis rate can also be affected by mixing with other substances, including other lactones and lactides [50].

PCL is approved by the Food and Drug Administration because of its natural biocompatibility and biodegradability and it causes only mild undesirable side-effects. PCL is widely studied for its application in medicine as a matrix for drugs with controlled long term release and long-term implants. Although PCL is especially suitable for wound dressings, tissue engineering and dentistry, it also has applications in the environmental sciences and food-packing industries [50, 51].

5. Electrospun artificial materials with attached nanoparticles for medical application

Long-term chronic wound healing is beset with the problem of infection because bacterial infection slows fibroblast proliferation and development and impairs rapid wound repair. Antibiotics are widely used to combat these infections, but indiscriminate use has led to resistance, and dressings with localised anti-bacterial delivery are now essential. Novel artificial wound dressings such as those containing Ag NPs can now accelerate chronic wound healing and combat microbial infection [30, 38].

The function of antibacterial agents, including Ag NPs, is best achieved by:

(1) mixing the agent(s) with polymer solution to create a bioactive composite,
(2) modifying the entire fibre web surface after electrospinning, or
(3) coaxial electrospinning.

The electro-spun materials are now investigated because of their structural similarity to the dermal extra cellular matrix [30, 38].

Figure 13 shows an example of Zang et al's [52] results from coaxial electrospinning to obtain core-shell PCL/collagen fibres. These are homogeneous without beads and have porous structure with average 200-400 nm fibre diameter.

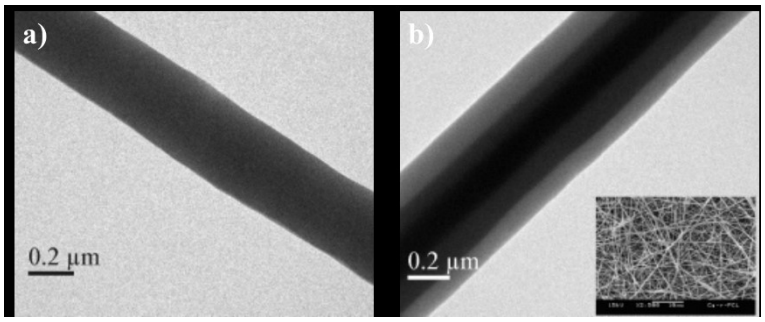

Figure 13: TEM image of prepared composited fibers; a) PCL fiber and b) PCL fiber coated by a collagen shell; scale bar 0.2 µm [52].

This study proved that PCL nano-fibres coated with collagen reliably imitated the natural extra cellular matrix, and had better properties than fibres with individual components. Cells easily adhered to the PCL/collagen fibres and the authors suggest that these core-shell nano-fibres have promise for tissue engineering [52].

Mohseni et al. [11] then studied PCL/PVA nano-fibres as a wound dressing containing silver sulfadiazine and Ag NPs reduced by chitosan. The homogeneous solution had 10 wt% PCL at Mw = 80,000 g·mol^{-1}, and it was dissolved in 1:1 chloroform/methanol solvent and stirred for 3 hours at room temperature. They optimised the electrospinning process at 3 mL/h flow rate, 27 kV electric potential and 1000 rpm rotating collector speed to obtain uniform PCL nanofibers.

The authors prepared PVA as the Ag NP/silver sulfadiazine carrier. They stirred 10wt% PVA at Mw = 72,000 g·mol^{-1} in distilled water for 4 hours at 8 ºC, and added Ag NPs and silver sulfadiazine at different concentrations. The electrospinning was set to 1 mL/h flow rate, 21 and 25 kV electric potentials and 1000 rpm rotating collector speed [11].

Increasing Ag NP concentration led to decreased average PVA fibre diameter due to increased electrical conductivity in the polymer solutions. In contrast, silver sulfadiazine addition increased average PVA fibre diameter; most likely because of high Mw and low silver sulfadiazine polarity. Figure 14 highlights the homogeneous Ag NP dispersion loaded in the PVA fibres [11].

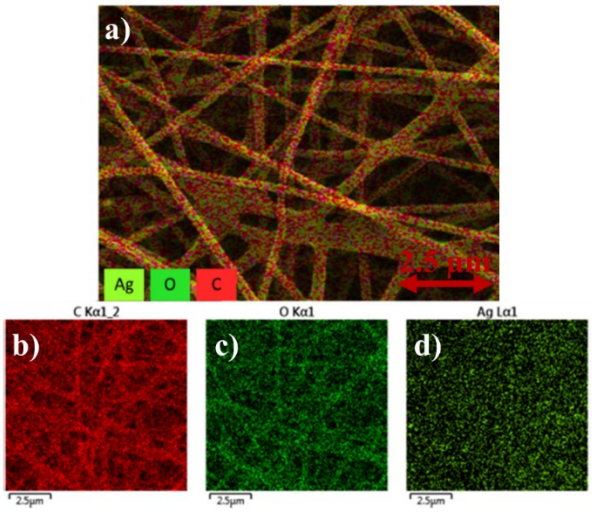

Figure 14: Elemental mapping analysis of PVA fibers a) loaded by Ag NPs: b) element C, c) elemenet O and d) element Ag; at 2.5µm scale bar [11].

The authors compared Ag NPs and sulfadiazine antimicrobial effect against *Staphylococcus aureus* (*S. aureus*) bacteria. No obvious differences were observed when high Ag NP concentrations or sulfadiazine were used [11]. The material biocompatibility was then evaluated by MTT cytotoxicity assay, and this proved that Ag NPs had faster

healing rate than fibres loaded with silver sulfadiazine. This was most likely due to the higher biocompatibility witnessed in the cytotoxicity study, and the silver sulfadiazine also caused greater toxicity to fibroblast cells at similar concentration [11].

These results were supported by Liu et al. [53] and Qian et al. [54] in clinical studies where they compared Ag NP and silver sulfadiazine efficiency. The studies confirmed that Ag NP was a more promising antimicrobial agent than silver sulfadiazine.

A most important study was then performed by Hassiba et al. [44] who prepared an electro-spun double-layered nanocomposite material for wound dressings. This comprised an upper fibrous PVA/ chitosan layer containing Ag NPs and a lower fibrous mat composed of PEO or PVP loaded with chlorhexidine. The upper layer with Ag NPs protected the wound from environmental germ invasion and the lower layer of antibiotics helped to prevent infection and accelerate wound healing. The upper PVA/chitosan/Ag NPs layer alone had antibacterial activity. Its connection with the lower PEO/PVP/chlorhexidine layer then enhanced this antibacterial effect [44].

Experimental part

6. Materials and methods

6.1. Synthesis of silver nanoparticles

Preparation of Ag NPs by individual organic compounds was chosen here for reproducibility and to elucidate the phytosynthesis process. Based on lack information in the literature about synthesis Ag NPs by maleic acid (MA), material availability and chemical structure of the molecule, this substance was chosen for diploma thesis. Figure 15 indicates that the cis form of MA is an inorganic unsaturated dicarboxylic acid, and the trans form is called fumaric acid [55].

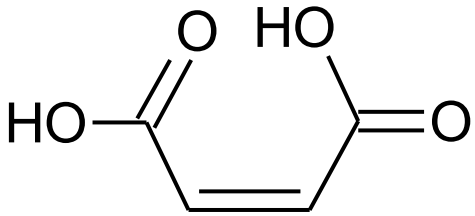

Figure 15: Cis-butenedioic acid recorded in IUPAC.

The Ag NPs were synthesised using MA ($C_4H_4O_4$, Mw = 116.07 $g \cdot mol^{-1}$, ≥ 99 % purity, Carl Roth) and silver nitrate ($AgNO_3$, Mw = 169.88 $g \cdot mol^{-1}$, ≥ 99 %, Carl Roth). The following MA concentration lines were then prepared to establish the boundary where Ag NPs synthesis does not occur**:** 10, 1, 0.1, 0.01 and 0.001 $mmol \cdot dm^{-3}$ (mM). The 10 mM $AgNO_3$ precursor was then added in 1:1 ratio to each acid solution, and Ag NPs were kept at 4 °C in the dark for further use.

The prepared samples were labelled in the following decreasing maleic acid concentrations: 10MA-Ag, 1MA-Ag, 0.1MA-Ag, 0.01MA-Ag and 0.001MA-Ag. Samples were then characterised by X-ray diffraction, TEM, ζ-potential and dynamic light scattering.

6.2. Preparation of the poly(ε-caprolacton) fibre matrix

The PCL water-insoluble polymer was chosen for the fibre matrix preparation because these fibres have better mechanical properties, such as strength, than PVA fibres. Its slower degradation time should also provide wound protection from airborne bacteria. Unfortunately, PCL could not be used to encapsulate the prepared Ag NPs because of its insolubility in aqueous colloidal solution as was mention in chapter 4.3.1.

The PCL with average 80,000 $g \cdot mol^{-1}$ Mw was obtained from Sigma-Aldrich (USA). This was stirred at 150 rpm in a 4:1 chloroform/methanol solution to final 10 wt% concentration and kept over-night at room temperature.

Figure 16 shows the Nanospider NS 1WS500U (Elmarco, Czech Republic) equipment used for PCL fibre matrix preparation at the Department of Nonwoven and Nanofibrous materials at the Czech Technical University of Liberec. The experiment was performed at 22.9 °C and 36.5 % humidity, and the distance between the 10 kV negatively charged collector and the 50 kV positive electrode was 16 cm. The PCL fibres were formed on a spun-bond with the substrate-shift set at 14 mm/min.

Figure 16: The Nanospider NS 1WS500U used in PCL fibre matrix preparation.

6.3. Anchoring the silver nanoparticles to the fibre matrix

Here, the water-soluble PVA polymer was chosen as the Ag NP carrier because NPs were prepared in aqueous colloid solution (chapter 4.2.1). Most importantly, PVA rapid dissolution on contact with human moisture produces immediate release of the antibacterial Ag NPs to wounds [17, 45].

The PVA from Sigma-Aldrich (Mw = 9,000–10,000 $g \cdot mol^{-1}$, 80 % hydrolysed) was used to prepare the 10 wt% of PVA and 10 wt% PVA+Ag solutions. The PVA was dissolved in distilled water to obtain PVA solution, and the PVA+Ag sample was prepared in Ag colloid using preliminary biosynthesis at 23 °C room temperature and 2 hours magnetic stirring.

The electro-spraying was done by 4SPIN® (Contipro, Czech Republic) in PrimeCell Bioscience at Ostrava. The PVA and PVA+Ag solutions were placed in a 10 mL poly(vinyl chloride) syringe with 0.8 mm stainless steel needle. The C1 static collector was covered with aluminium foil or previously prepared PCL fibres. Control samples of the droplets collected on aluminium foil were prepared for 30 minutes: PVA_30 and PVA+Ag_30. They served for evaluating droplets morphology, size distribution and to optimize the process. Final samples sprayed at PCL matrix were obtained at optimised 25 kV applied voltage 10 µl/min flow rate and 18 cm collector-emitter distance. The PVA control samples were sprayed for 60 minutes and labelled PCL/PVA_60, and the PVA+Ag materials were prepared at 15, 30, 45 and 60-minute spraying time to obtain gradually increasing Ag NPs concentration in the PVA droplets. Prepared PCL matrix with PVA+Ag were designated according to the spraying time as follows: PCL/PVA+Ag_15; PCL/PVA+Ag_30; PCL/PVA+Ag_45 and PCL/PVA+Ag_60. All experiments were conducted at 23 °C laboratory temperature and approximately 36 % humidity.

7. Characterisation methods

7.1. Electron microscopy

Micrographs from transmission electron microscopy (TEM) were obtained after 24 hours from precursor and MA mixing and NPs formed in the solution were observed. Ag NPs morphology and size distribution were characterised by JEOL 1011 (JEOL, Japan) at the Faculty of Science at Charles University in Prague. The 2 μl of sample was applied onto carbon/formvar grids and sample characterisation was possible after 10 minutes of air-drying. TEM images were then post-processed by JMicroVision software and minimum of 500 Ag NPs were then evaluated to get size distributions parameters for each sample. The histogram of the means of the sizes was then created in MATLAB software.

Scanning electron transmission microsope (STEM) JEOL JSM-7610F Plus was used for image analysis. The droplets and fibrous samples were characterised by SEM at 15 kV applied voltage (JEOL, Japan). This characterisation consisted of Secondary Electron Detector (LEI), the Back-Scattered Electron Detector (COMPO) and the Energy Dispersive Spectroscopy micro-analyser (Aztec Ultim MAX - EDS, Oxford Instruments, GB). The samples were sputtered with a thin 20nm layer of platinum by the ultra-fine Q150V Plus coater (Quorum Technologies, UK). The electro-spun droplet/fibre size distribution was evaluated in image analysis by the JMicroVision program. At least 250 average fibre diameters and 500 droplet diameters from the STEM micrographs of each sample were contained in the image analysis, and histograms were created in MATLAB software.

Also, using transmission mode (STEM) at 30 keV on STEM JEOL JSM-7610F Plus further development of NPs formation/aggregation 14 days after precursor and MA mixing was controlled.

7.2. X-ray diffraction (XRD)

100 μL of colloidal sample were five times applied on microscopic slide and dried at 50 °C for 30 minutes to obtain a representative thin layer of the sample on glass plate.

The XRD patterns were recorded by Bruker D8 DISCOVER diffractometer (Bruker AXS, Billerica, USA) equipped with an X-ray tube with rotating Cu anode at λ=1.5418 Å and 12 kW. All measurements were performed in parallel beam geometry with a parabolic Goebel mirror in the primary beam. The X-ray diffraction patterns were finally recorded

in grazing incidence in 2 theta range from 5 to 80° with 0.05° step-size and α=1.5° angle of incidence.

7.3. Chemical-physical characterisation of colloids and polymer solutions

The Ag NPs size distribution was assessed by ZetaSizer Nano–ZS dynamic light scattering (DLS, type ZEN 3600; Malvern Instruments Ltd., UK). The DLS analysis was conducted in a plastic cuvette cell with 2 mL of NPs solution, and ζ-potential was controlled in the ZetaSizer Nano–ZS by laser Doppler velocimetry. This system applies an electric field to the disposable ζ-potential cell with approximately 2 mL of sample and it measures the particle motion by electrophoretic light scattering. The ζ-potential values establish the electrostatic stability of the tested solutions. Colloidal sample pH was measured according to ČSN ISO 10523.

The viscosity of the homogenous PVA and PVA+Ag solutions was measured by DV2T Viscosimeter (Brookfield Ametek, USA), and dynamic viscosity was determined from the magnitude of the torque measured in steady-state rotation. This was set at appropriate SC4-18 spindle speeds in the SC-13R sample container.

7.4. Antibacterial activity

The prepared materials' (PCL, PCL/PVA_60, PCL/PVA+Ag_15, PCL/PVA+Ag_30, PCL/PVA+Ag_45, PCL/PVA+Ag_60) antibacterial activity against bacterial culture *S. aureus* CCM 299 and *E. coli* CCM3954 was evaluated. Both cultures were obtained from Collection of Microorganisms (Brno, Czech Republic). Fibrous materials were cut into required squared shapes and placed to Eppendorf tube with bacterial solutions. After 2, 3, 6, 12 and 24 hours the bacterial suspensions were removed from the Eppendorf tube and placed on blood agar plates and then evaluated. Antibacterial testing has occurred in cooperation with University of Veterinary and Pharmaceutical Sciences Brno (Czech Republic).

7.5. Cytotoxicity testing

The PCL, PCL/PVA_60, PCL/PVA+Ag_60 fibrous samples were cut to the required diameters and sterilised by UV lighting for three hours from each side.

The preparation of Vero Cells (passage 44, African Monkey Kidney, ATCC, USA) was identical for both tests. The cells were cultivated in Minimum Essential Medium with Earle´s Salts (EMEM; Biowest, France) and supplemented with 10% v/v foetal bovine serum (FBS; Biowest, France). A 2 mL suspension of Vero cells were then removed from the culture flask by enzymatic digestion (trypsin/EDTA, Sigma-Aldrich, USA) and the cell suspension was centrifuged. Finally, the cells were re-suspended in culture medium at $1x10^5$ cells/mL density.

Direct-contact test and MMT assay herein were performed in cooperation with Public Health Institute Ostrava in accordance with ČSN EN ISO 10993-5.

- Direct-contact test

Prepared 1x1 cm quantities of sterile material were placed to the centre of a 6-well plate in duplicate and loaded with stainless-steel weights to prevent material movements. Then 2 mL of prepared Vero cell suspension was seeded into 6-well plates (= $2x10^5$ cells/well plate) with samples. The cells were incubated for 24 and 48 hours in incubator (5 % CO_2, T=37 °C, > 90 % humidity). Qualitative cytotoxicity evaluation was then conducted on morphology, vacuolisation, detachment, cell lysis and membrane integrity using optical microscope Olympus CKX41 (Olympus, Japan).

- MTT assay

Samples were cut to the required 6 cm^2 surface area, and culture medium with 10 % v/v FBS was used for extraction because of its ability to support cellular growth and extract both polar and non-polar substances. This extraction was performed 24 hours at 37 °C in using sterile containers and aseptic techniques.

Here, 100 µL of Vero cell suspension was seeded into 96-well plates at $1x10^4$ cells in each well. The cells were incubated for 24 hours in incubator (5 % CO_2, T=37 °C, > 90 % humidity) and they formed a semi-confluent monolayer. The medium was aspirated from the cells after incubation, and 100 µL of the treatment medium was added. This contained the given extract concentration with positive latex (PC) or negative polystyrene controls (NC) added to the cell culture plates. The extract concentrations were 100, 50, 25 and 12.5 % v/v.

After mixing, the cells were first incubated for 24 hours (5 % CO_2, T=37 °C, > 90 % humidity), and the culture medium was then removed from the plates and 50 µL of the MTT solution (3-(4,5-dimethylthiazol-2-yl)-2,5-diphenyltetrazoliumbromid, 1 mg MTT/mL complete medium, Sigma-Aldrich, USA) was added to each well. The plates were incubated for 2 hours in the incubator (5 % CO_2, T=37 °C, > 90 % humidity). Finally, the MTT solution was decanted and 100 µL of isopropyl-alcohol was added to each well to dissolve the formazan crystals formed in the cells.

The plates were shaken for a short time by plate-shaker, and the absorbance was measured using a 570 nm filtered microplate reader. The cell viability was then calculated from the mean MTT of the three replicate values in each test concentration. This value was compared to the mean MTT value of all blank controls, and relative cell viability was finally expressed as a percentage of the control values.

8. Results and discussion

8.1. Silver nanoparticle morphology and size distribution

Ag NPs were successfully prepared when all MA solutions were mixed with the silver precursor, and TEM analysis confirmed the presence of mostly spherical Ag NPs in all samples. Hexagonal Ag NPs were also present in the samples, but to a lesser extent. There were no significant differences in size distribution in the studied samples, with the following average Ag NPs dimeters established; 8 ± 5, 6 ± 3, 8 ± 3, 8 ± 4 and 6 ± 3 nm for MA decreasing 10,1, 0.1, 0.01 and 0.001mM concentrations, respectively.

Evaluation indicated a narrow range of size distributions for each MA concentration. Larger 3 nm diameter nanoparticles were also present in 10MA-Ag and 0.1MA-Ag samples, but in much smaller number. Figure 17 histograms depict the average sizes and divergences.

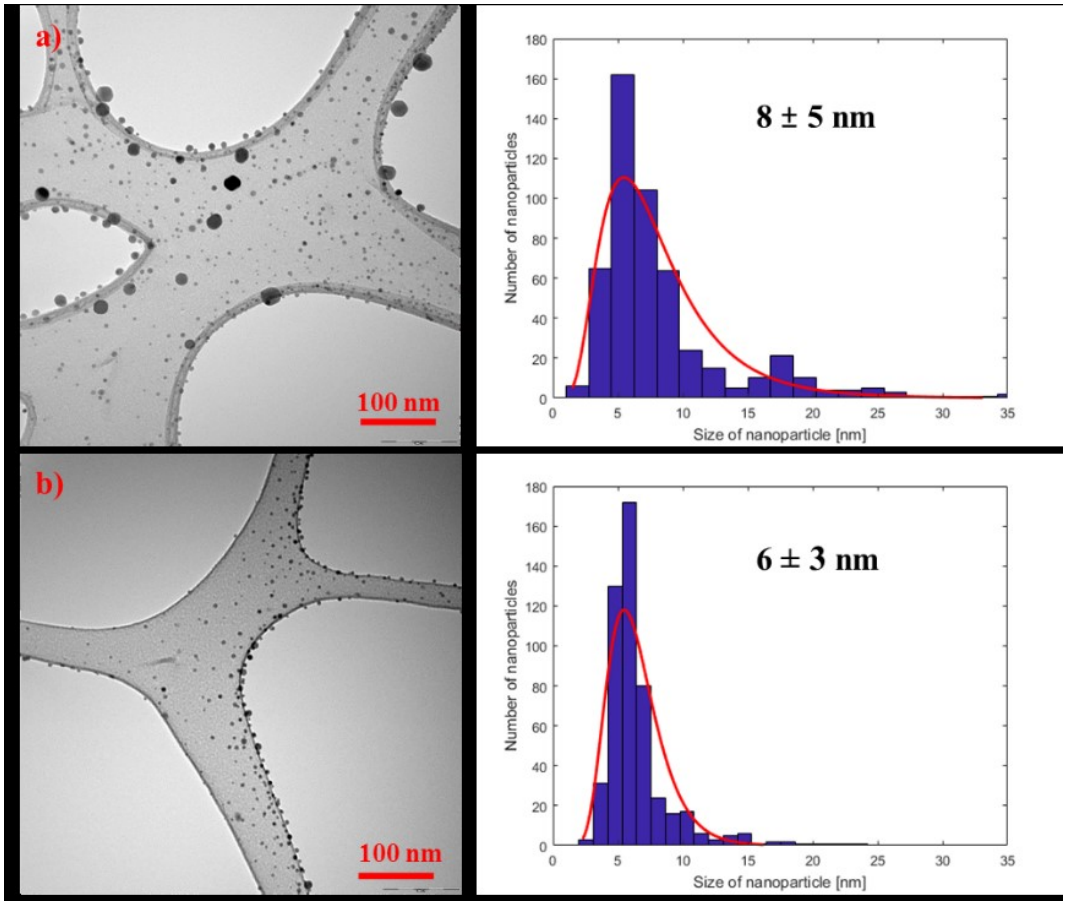

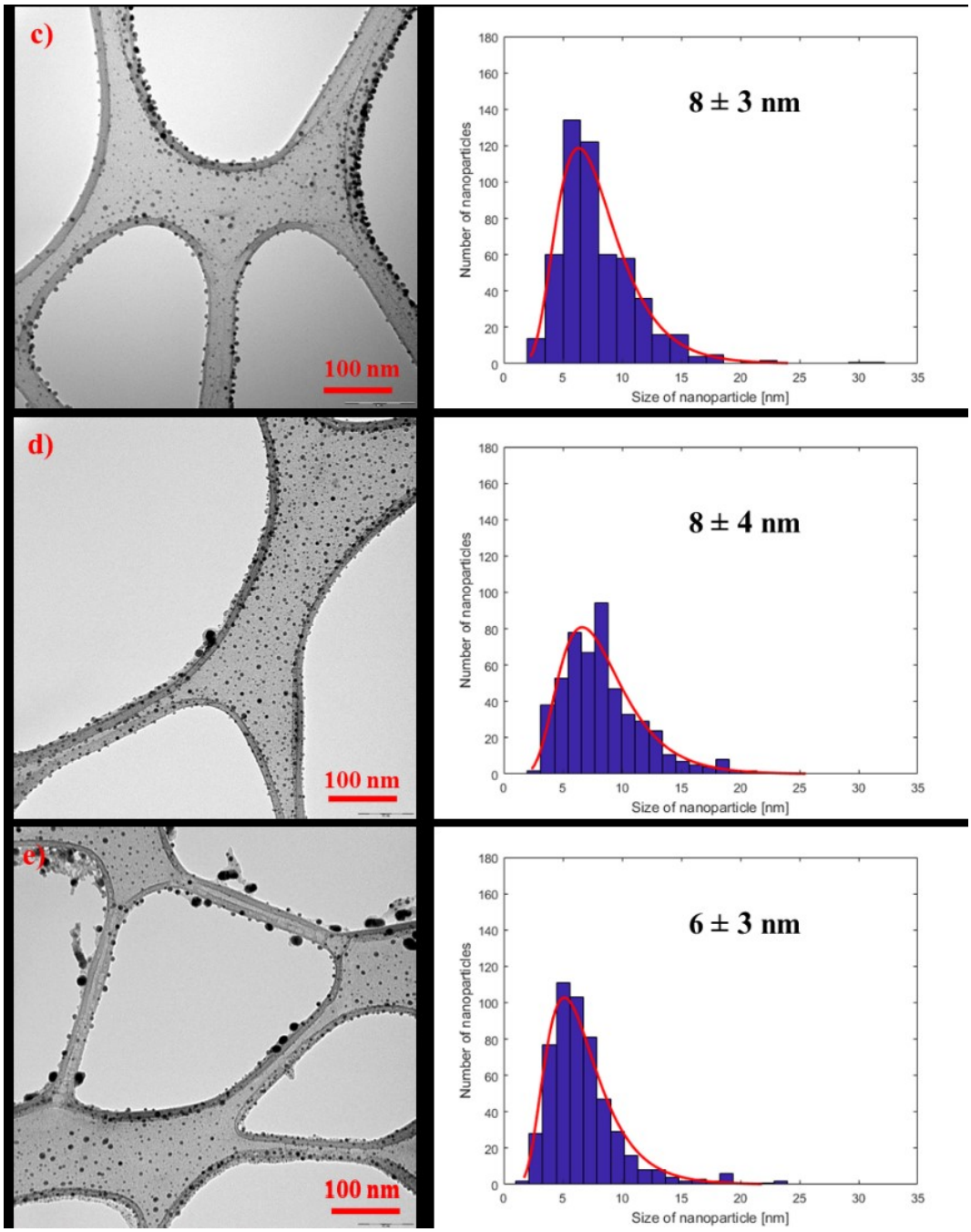

Figure 17: TEM images of Ag NPs samples and their histograms: a) 10MA-Ag, b) 1MA-Ag, c) 0.1MA-Ag, d) 0.01MA-Ag and e) 0.001MA-Ag. Difference in shapes or size distributions of Ag NPs were not observed; scale bar 100 nm.

Contrast to NPs prepared by mixtures of phytochemicals such as leachate [17] and extracts [26, 31] the use of one standard phytochemical substance didn´t led to the formation of a significant stabilising cover around the NPs, however, it is known that some phytochemicals have both functions - reduction and stabilisation [33]. A weak

stabilisation covers around NPs were detected for each sample and as an example it can be observed in Figure 18.

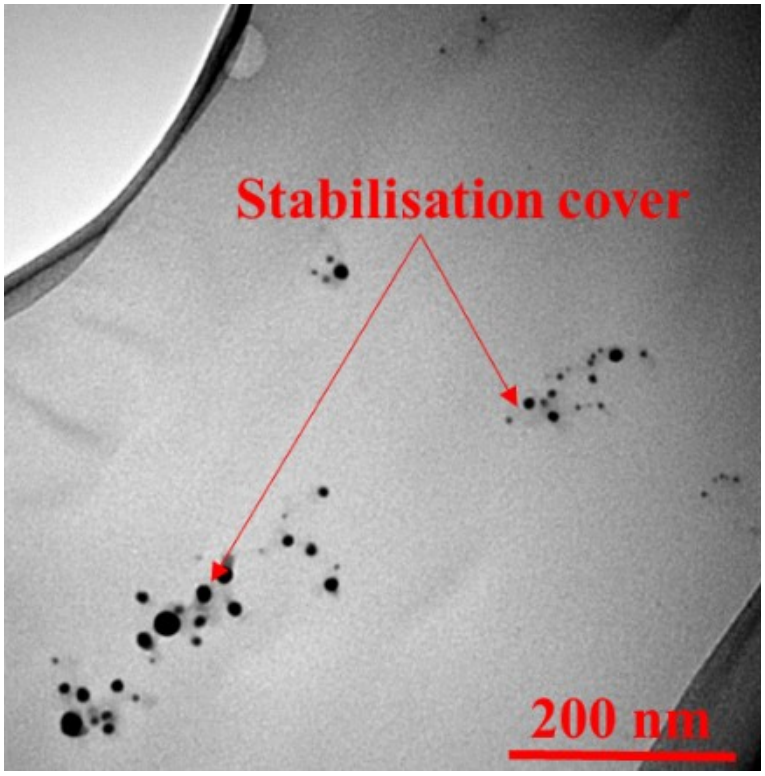

Figure 18: Sligh stabilization cover detected by TEM in the sample 1MA-Ag.

The Ag NPs size distributions were measured by DLS. They were determined for decreasing MA concentration in this order: 224 ± 31, 134 ± 11, 185 ± 9, 89 ± 10 and 50 ± 12 nm (Table 2).

Table 2: Evaluation of size distributions for each MA concentration measured by DLS and TEM image analysis.

Sample	DLS		TEM
	Range of NPs sizes [nm]	Diameter [nm]	Diameter [nm]
10MA-Ag	110 - 480	224 ± 31	8 ± 5
1MA-Ag	60 - 350	134 ± 11	6 ± 3
0.1MA-Ag	110 - 310	185 ± 9	8 ± 3
0.01MA-Ag	29 - 410	89 ± 10	8 ± 4
0.001MA-Ag	25 - 265	50 ± 12	6 ± 3

TEM size distribution was then compared to DLS analysis, and significant differences were observed. While DLS analysis established the average hydrodynamic diameters, the TEM image analysis provided the "core diameter" average [17]. It is widely accepted that this measurement method includes the thickness of compounds covering NP's surface and the great size range measured in DLS analysis may also be influenced by crystals and aggregates confirmed by TEM. Crystals were detected in samples 10MA-Ag and 1MA-Ag (Figure 19). The formation of aggregates was observed in all colloidal mixtures.

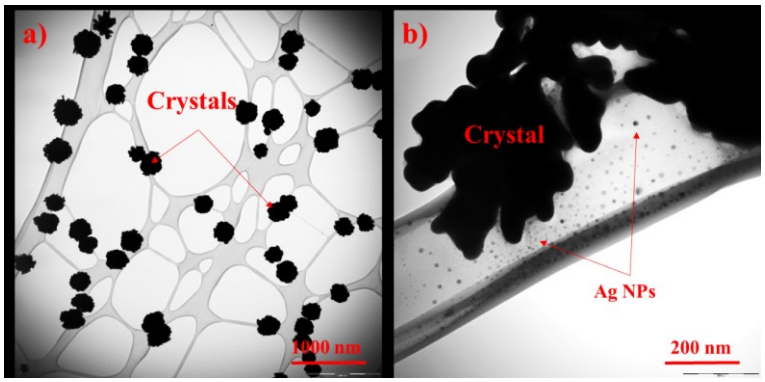

Figure 19: TEM images of a) the crystals and b) Ag NPs 6 ± 3 nm in the 1MA-Ag sample; scale bar 1000 and 200 nm.

8.2. X-ray diffraction analysis

Colour changes were observed during sample preparation for XRD analysis. Here, Figure 20 a) and b) show that the 10MA-Ag and 1MA-Ag samples formed white crystals compared to the dark-brown staining observed in the remaining Figure 20 c), d) and e) samples. The difference between these samples were further confirmed by XRD.

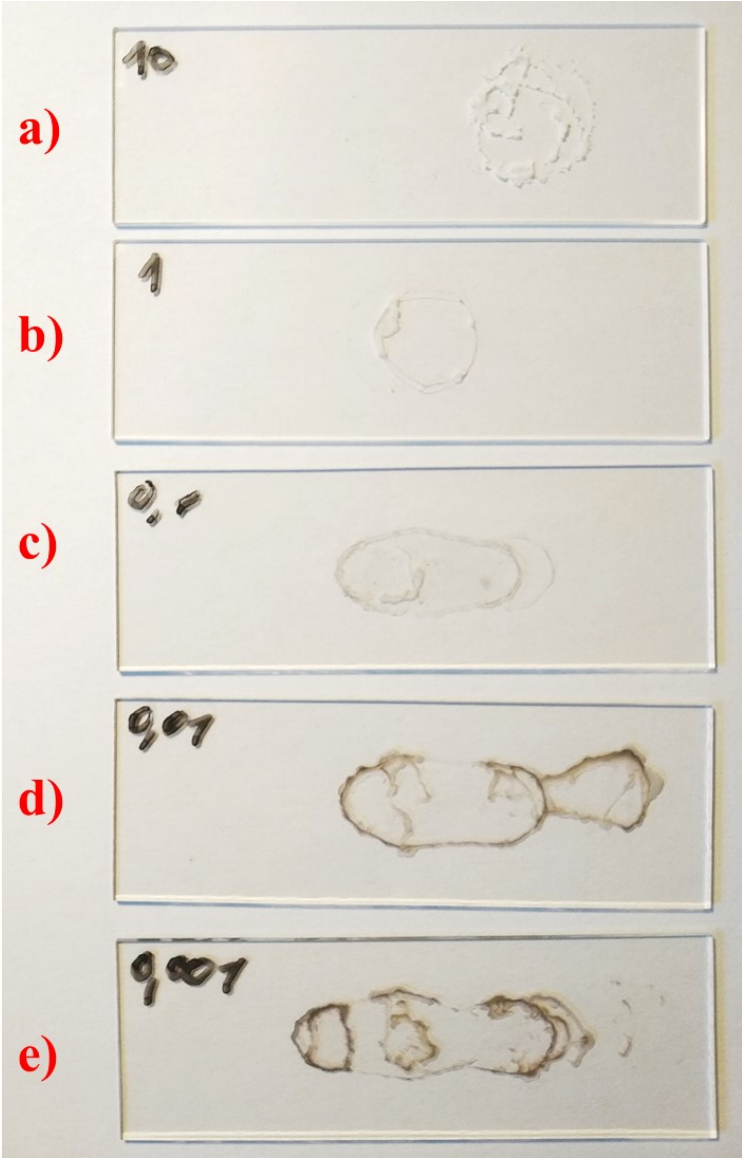

Figure 20: Prepared Ag NPs samples for XRD analysis: a) 10MA-Ag, b) 1MA-Ag, c) 0.1MA-Ag, d) 0.01MA-Ag and e) 0.001MA-Ag. The different colouring indicates the change between samples.

Figure 21 shows the difractogram of the prepared samples. This confirmed the differences observed during their preparation and drying. The 10MA-Ag and 1MA-Ag

samples had peaks at approximately 10° to 15° on the 2-theta scale, and these could correspond to organic residues (MA residues and/or MA -oxidized products or intermediates). Chemical redox interactions took place, when MA and $AgNO_3$ were mixed and Ag NPs began to form, however, some new (secondary) phases of organic origin could be observed/identified in the difractogram. From more complex insight, coordination polymers with silver [55], which may be metastable and may disintegrate into Ag NPs or grow in time, correspond to this description. These complexes could be observable using TEM as well and are documented on Figure 22.

The middle 20° to 50° of the 2-theta-scale corresponds to the presence of orthorhombic and rhombohedral $AgNO_3$ crystals. This 2-theta range was most significant for 0.1, 0.01 and 0.001MA-Ag samples because $AgNO_3$ predominates there, and this aligns with physical-chemical measurements. It is therefore considered that the 0.1, 0.01 and 0.001 mM MA concentrations were too small to quantitatively react with the applied 10 mM $AgNO_3$.

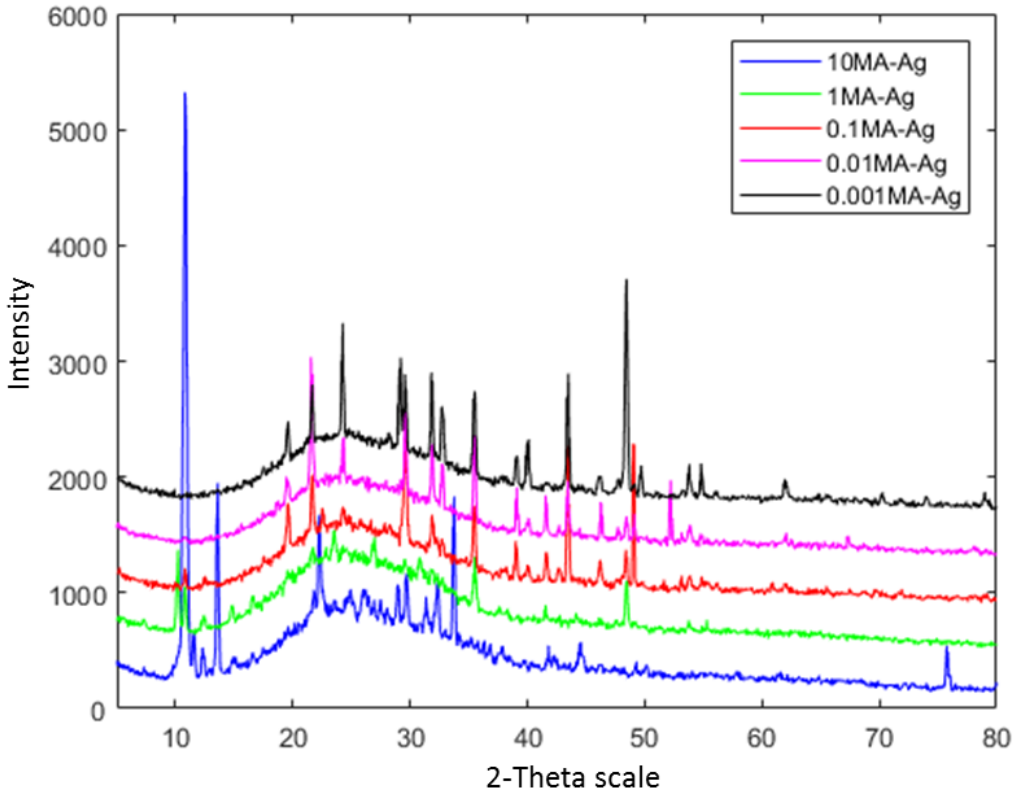

Figure 21: The difractogram of Ag NPs colloid samples.

The cubic (111), (200) and (220) Ag NPs forms usually detected at approximately 38°, 44°, 64° and 77° on the 2-theta scale [17] and observed in TEM images were unfortunately not confirmed by XRD analysis. However, this may be because significant organic residue crystals present in 10MA-Ag and 1MA-Ag samples or significant $AgNO_3$ extant in others three samples, and the signal is stronger in those sample analyses than in small amount of Ag NPs with diameters in units of nanometres.

As was mention previously, mostly spherical Ag NPs were observed in all samples, and Figure 19 and Figure 22 show that 10MA-Ag and 1MA-Ag sample images contained the large crystals probably of metastable organic residue.

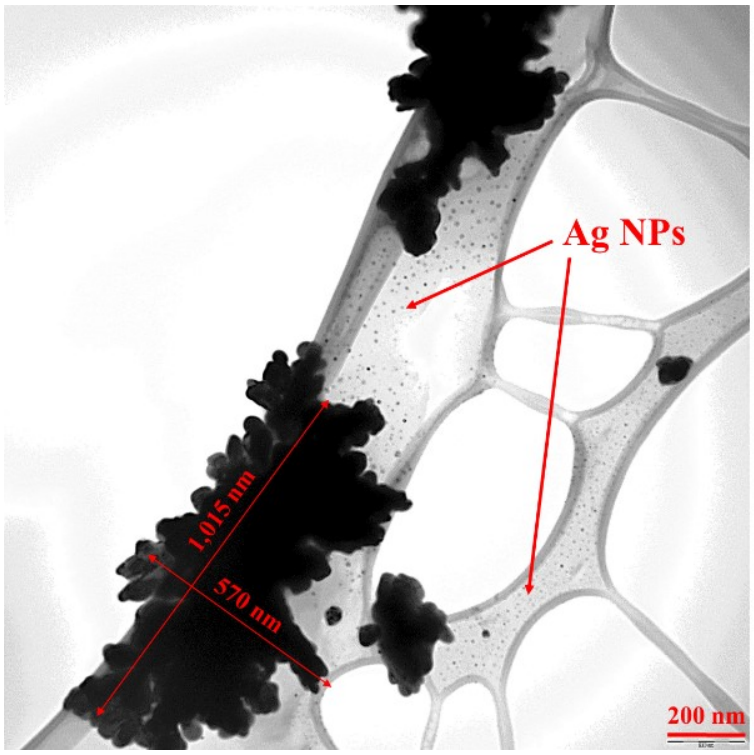

Figure 22: TEM image of crystals present in sample 10MA-Ag. Synthetized Ag NPs 8 ± 5 nm were also detected.

Although the available literature does not clarify the MA and silver ion synthesis mechanism, results highlight that the -OH functional groups in MA could cause reduction of Ag^+ ion to Ag NPs. Here, the $AgNO_3$ metal precursor dissociated in water to Ag^+ and NO_3^- ions. The -OH functional group in the dicarboxylic MA acid then reacted with the Ag^+ ion and cleaved the H from the OH group, and a silver ion interacted with the negatively charged O^-.

The double-bonded O in MA also gains negative charge (free electron pair), and researchers consider that this O also participates in forming the complex [55]. Thus, the individual MA molecules' interaction with silver ions formed a meta-stable complex which may subsequently disintegrated to Ag NPs (Figure 23). However, the description of the formation and disintegration of the complex requires confirmation.

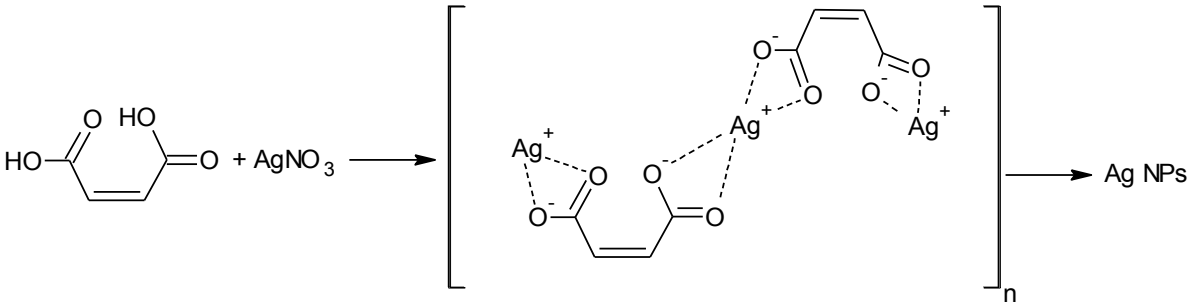

Figure 23: Possible mechanism of meta-stable complex formation, which subsequently disintegrated to form Ag NPs.

8.3. Stability of silver nanoparticles

A ζ-potential value above ± 30 mV generally describes a stable system, but stability especially depends on pH provision sufficient charge to confirm colloid stability [56].

The negative ζ-potential value of the colloidal Ag NPs was measured for each sample and these were determined for decreasing concentration in this order: -1.3, -3.7, -4.3, -3.1 and -3.4 mV (Table 3). All samples appeared unstable the ζ-potential values proved too low to achieve theoretical boundary value and there was a tendency for aggregation and agglomeration when the samples were measured at laboratory temperature. However, these processes were not been shown in TEM analysis or probably system is not on equilibrium after a short period of three days and a lot of ions in the mixture are still in the redox process.

Table 3: Value of the ζ-potential and pH of Ag NPs colloidal system for each sample.

Sample	ζ-potential [mV]	pH
10MA-Ag	-1.3	2.5 ± 0.1
1MA-Ag	-3.7	1.9 ± 0.1
0.1MA-Ag	-4.3	2.6 ± 0.1
0.01MA-Ag	-3.1	3.4 ± 0.1
0.001MA-Ag	-3.4	4.3 ± 0.1

Colloidal system stabilization can be affected by pH value, and this was therefore measured for each sample (Table 3). The samples' acidity was confirmed. They were determined for decreasing concentration of MA in this order: 2.5, 1.9, 2.6, 3.4 and 4.3 ± 0.1. Samples with a higher MA concentration exhibited greater acidity, and the 10MA-Ag sample had a pH 2.5. In contrast, the pH increased to 4.3 with decreasing MA concentration and samples acquired neutrality.

These results suggest that it is necessary to continue optimising the physico-chemical properties so that the NPs in solution stay stable even under ambient conditions. For example, Jain and Mehata [31] studied the effect of adding NaOH to Ag NPs colloid prepared by quercetin. They confirmed higher stability at pH 10 when investigating pH changing in the 7 to 11 range. Although this indicates that MA could be an Ag NPs reducing agent, system stability most likely still requires altered pH.

Another important factor that is observed during synthesis is temperature and time. For TEM analysis after first 24 hours after mixing, samples were stored at 4 °C and NPs diameters were determined in units of nanometres. In contrast, other analysis required at least warming to room temperature (DLS) or higher (XRD).

Due to the instability of the system, the colloidal solutions were again analysed by STEM after 14 days. The previously observed particle spherical and hexagonal shapes and their presence were confirmed by analysis. Larger particle sizes were detected (Figure 24). Size distributions were determined for decreasing concentration in this order: 78 ± 22, 98 ± 31, 62 ± 20, 53 ± 22 and 78 ± 23 nm.

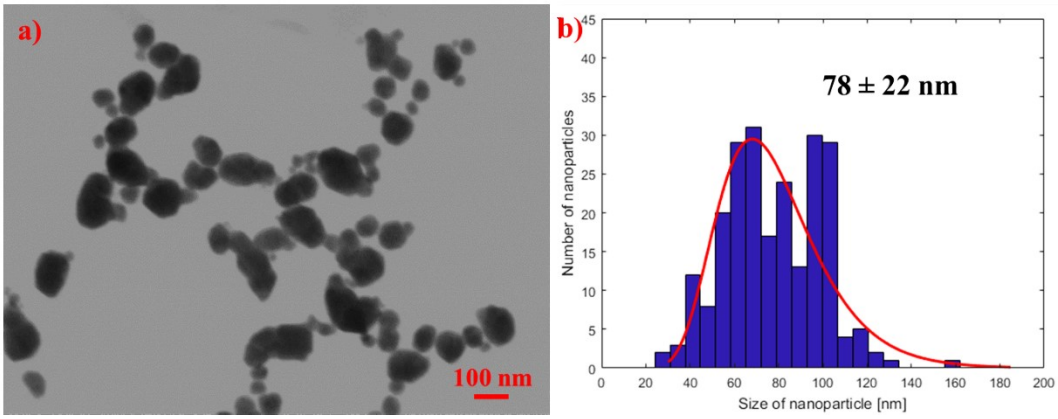

Figure 24: STEM micrograph of 10MA-Ag sample after 14 days from mixing MA and $AgNO_3$, where a) Ag NPs were confirmed with b) size distribution 78 ± 22 nm.

However, MA appears promising reducing agent but synthesis has to be further optimised, especially in the following purposes:

(1) to stabilise the system and focus especially on stabilising NPs by changing the pH or adding a stabilising agent,

(2) to determine the exact ratio between MA and $AgNO_3$,

(3) to analyse the formed crystals, because this could provide further clues to the synthesis mechanism.

A 0.1MA-Ag sample was chosen for the subsequent application, where mostly spherical Ag NPs with size distribution 8 ± 3 nm. Although this sample indicated $AgNO_3$ excess, the undetermined organic crystals observed in the 10MA-Ag and 1MA-Ag samples were not obvious. The negative value of ζ-potential was determined -4.3 and pH was 2.6 ± 0.1. The sample 0.1MA-Ag was then mixed with the PVA to obtain 10 wt%

of polymeric solution and immediately electrosprayed to PCL fibrous matrix. This should resulted to the encapsulation and stabilization of small Ag NPs, which are more suitable for the intended application in medicine.

8.4. Characterisation of polymer solution that act as silver nanoparticles carrier

The required viscometer torque must be approximately 70 % or greater. This was achieved by using 150 rpm speed for both measured polymeric solutions. Table 4 highlights that pure PVA then had 17.08 mPa·s viscosity and the PVA+Ag value decreased to 13.92 mPa·s.

Table 4: PVA and PVA+Ag viscosity measurment at different speeds.

Speed [rpm]	PVA		PVA + Ag	
	η [mPa·s]	Torque [%]	η [mPa·s]	Torque [%]
130	16.96	73.5	-	-
140	16.99	79.2	-	-
150	17.08	85.4	13.92	69.6
160	-	-	13.89	74.1
170	-	-	13.92	78.9

The Ag NP presence is most likely responsible for the overall polymer viscosity value decrease from 17.08 to 13.92 mPa·s. This is supported by previous study [17] and further explained by Chou et al's molecular modelling of Ag NPs interaction with PVA [57]. This interaction of Ag NPs with PVA -OH groups and prevention of hydrogen bond formation between the individual PVA molecules could have decreased PVA+Ag viscosity. It is further possible that other compounds present in the colloid, such as $AgNO_3$, influenced the final viscosity. Unfortunately, the viscosity values could not be compared with other studies because this parameter depends on all the following; polymer Mw, the mass concentration, filler and solvent and the measuring apparatus.

While the PVA_30 sample had 750 ± 685 nm average diameter droplets, and 685 nm dimeters were the most common, the PVA+Ag_30 droplets had average 720 ± 635 nm diameter and approximately 610nm was observed most frequently. The PVA+Ag droplets were therefore smaller in diameter than the pure PVA droplets and they also had greater homogeneity and a slight tendency to fibre formation (Figure 25b). Finally, very large droplets over 1,500 nm were also noted, and Figure 25 herein presents the average sizes and deviations on histograms.

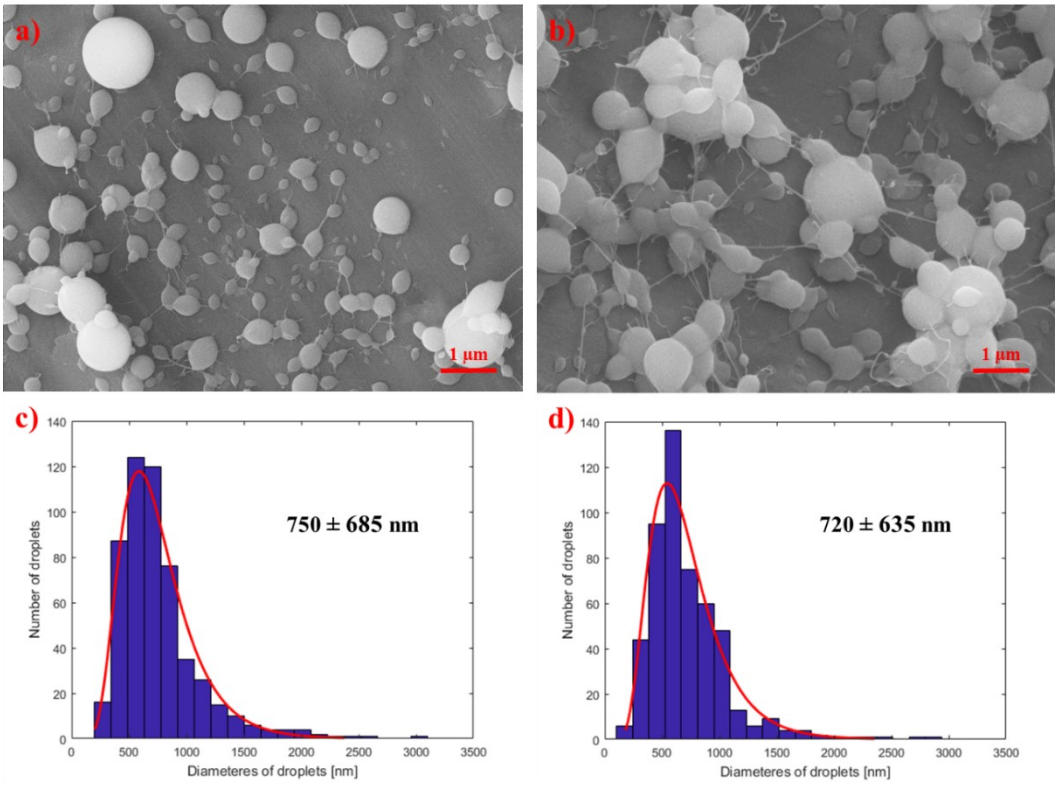

Figure 25: SEM images of droplets prepared from different polymer solutions a) PVA and b) PVA+Ag. . There was no great difference in droplet size distribution observed: c) sample PVA_30 and d) PVA+Ag_30 sample; scale bar 1 µm.

8.5. Poly(ε-caprolacton) fibre function as a droplet matrix

SEM analysis of PCL fibres confirmed successful preparation of fibres with average 2,066 ± 881nm diameter (Figure 26). However, the occasional larger fibre diameters above 3,500nm caused significant deviation in the calculated averages. The most frequently observed fibre diameter in the basic PCL matrix was approximately1,800 nm, and these PCL fibres were used as the basic matrix for electro-spraying the PVA and PVA+Ag polymeric solutions.

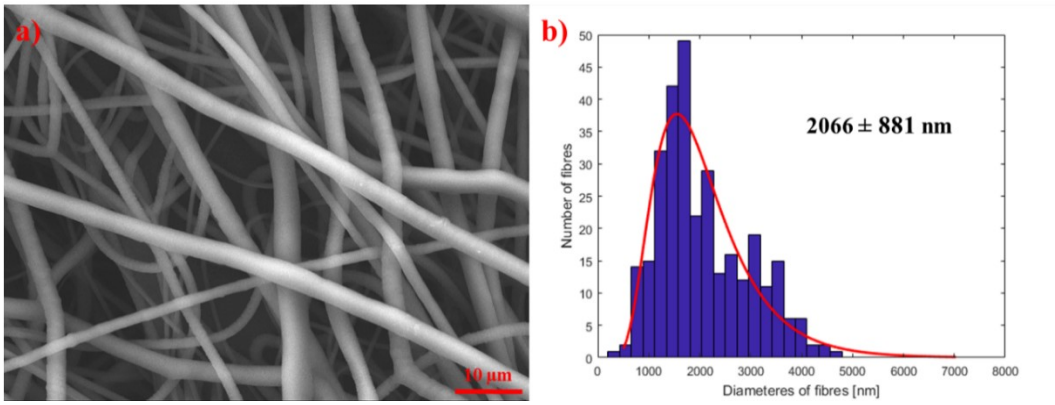

Figure 26: SEM image of a) PCL fibres prepared via Nanospider™ and b) their size distribution; scale bar 10 µm.

Figure 27 highlights the change in colour in the material during preparation of the samples for analysis. The samples prepared by spraying PVA+Ag turned orange after a month's storage, and this visual confirmation of Ag NPs droplets on the PCL fibres established that the fibres acted as an attachment matrix (Figure 27 c)-f)).

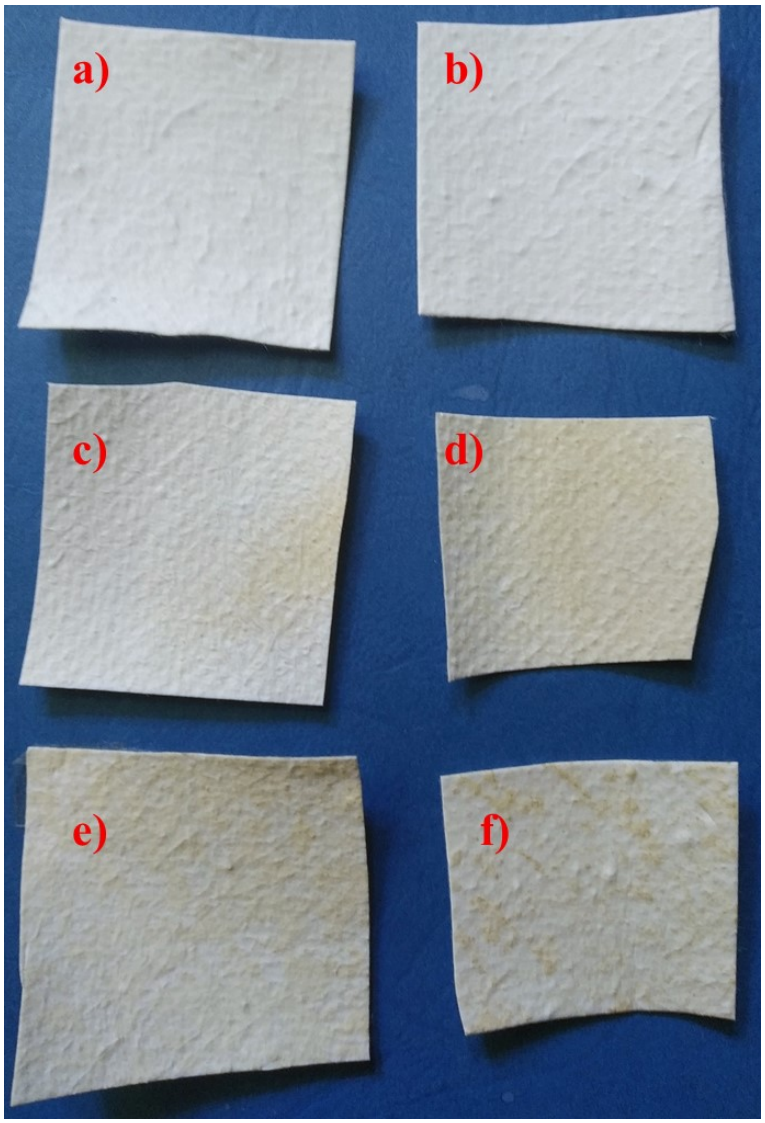

Figure 27: Visual differences in prepared fibrous sample colour: a) PCL fibres and b)PCL/PVA_60 as control samples are white and samples with Ag NPs sprayed for different time periods: c)15, d) 30, e) 45 and f) 60 minutes highlight colour change to orange.

Figure 28 shows that the electro-spraying of both PVA and PVA+Ag solutions on the PCL matrix was successful, and droplets in the sample were substantiated by SEM analysis. For example, the PCL fibre surface in Figure 28 a) was smooth compared to the samples with electro-sprayed PVA and PVA+Ag droplets, and Figure 28 b) provides evidence that the droplets were trapped on the surface of the fibres. Moreover, these droplets were also trapped in the fibre external layer.

The amount of PVA+Ag droplets sprayed on PCL fibrous matrix also depended on the length of spraying-time; 15, 30, 45 or 60 minutes (Figure 28 c)-f)). The number

of attached PVA+Ag droplets increased with longer electro-spraying time, so that sample PCL/PVA+Ag_60 contained the highest accumulation of PVA+Ag droplets

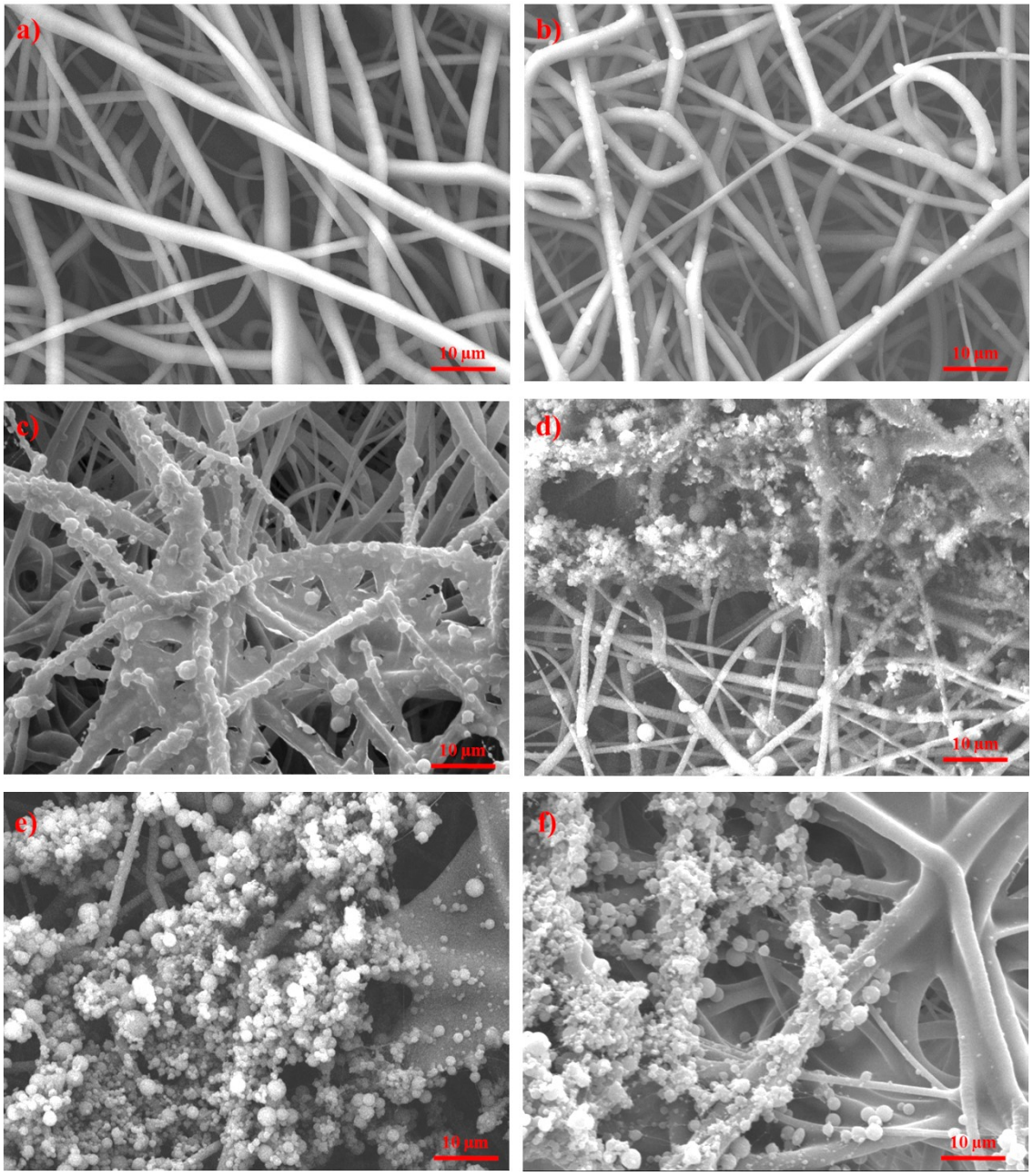

Figure 28: SEM images of prepared control samples: a) PCL fibres and b) PCL/PVA_60 with droplets on the surface and in the first PCL fibre layer. The Ag NPs prepared from 0.1 mM MA were encapsulated in PVA droplets and were applied for different lenghts of time: c) 15, d) 30, e) 45 and f) 60 minutes; scale bar 10 µm.

SEM and EDX analysis were applied to confirm the presence of Ag. The random Ag clusters visible in Figure 29 a) were most likely caused by applying electro-spraying process

parameters such as high voltage and inhomogeneity of droplets trapping on static collector. The C and O chemical elements form part of the PVA and PCL structures and the presence of Pt is caused by sputtering the samples for SEM analysis.

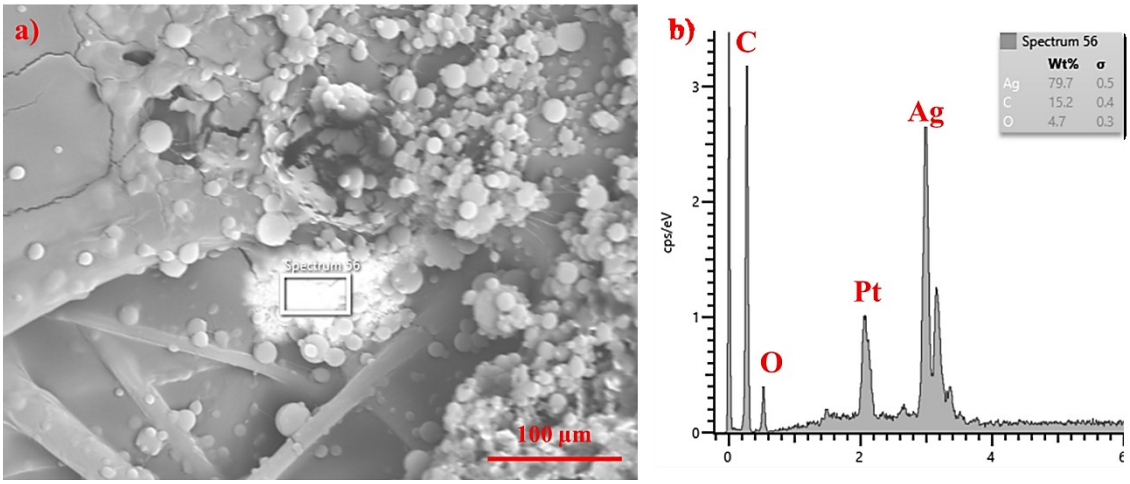

Figure 29: SEM image of a) the sample PCL/PVA+Ag_45 with droplets, PCL fibres and location of Ag and b) EDX analysis of chosen sample region; scale bar 100 µm.

8.6. Characterisation of prepared antimicrobial material

The Gram positive *S. aureus* and Gram negative bacteria *E. coli* are common bacterial strains used in antimicrobial testing. These bacterial strains established resistance to antibiotics, and alternative treatment for bacterial infections is urgent required [58].

Table 5 and Table 6 highlight the proven efficacy of Ag NPs attached to a fibrous matrix against *S. aureus* and *E. coli*. The lowest 15-minute electro-spraying time of PVA+Ag provided the least number of droplets with Ag NPs, but even this short period had proven antibacterial activity against S. aureus, but not against *E. coli*. In contrast, the PCL and PCL/PVA_60 fibres without Ag NPs provided no antibacterial effect on either bacterium. Moreover, the PCL/PVA+Ag_30 and PCL/PVA+Ag_45 samples had antibacterial activity against both bacterial cultures; and higher antibacterial effect was observed against Gram positive *S. aureus* than Gram negative *E-coli*.

The PCL/PVA+Ag_60 sample efficiency was most impressive. Inhibition of the growth of both bacterial species was evident 3 hours after incubation, and 100 % inhibition was achieved after 6 hours.

The effect of each tested sample on the bacteria is contained in Table 5 and Table 6, and these show that the Ag NPs had greater antibacterial activity against Gram positive *S. aureus* bacteria than Gram negative *E.coli.* This is also supported by other authors who researched Ag NP antibacterial activity. The reason for different susceptibility could be explain by structural differences of the both bacterial strains. Gram negative cells have a cell wall composed of an outer lipopolysaccharide membrane and an inner relatively thin peptidoglycan membrane of only 3 to 4 nm thickness. Whereas, the cell wall of the Gram positive type lacks an outer lipopolysaccharide membrane and the peptidoglycan layer is thicker approximately 30 nm. These structural differences, including the thickness and composition of the cell wall could explain why Gram positive *S. aureus* is less sensitive to Ag NPs than Gram negative *E. coli.* This result has been found in other studies focusing at the antibacterial activity of Ag NPs [24, 25, 44].

Table 5: Antibacterial evaluation of prepared control fibrous samples and fibrous materials with Ag NPs against S. aureus.

Sample	Incubation time				
	2 hours	3 hours	6 hours	12 hours	24 hours
	Growth inhibition (100 %)				
PCL fibres					
PCL/PVA_60					
PCL/PVA+Ag_15					
PCL/PVA+Ag_30				-	-
PCL/PVA+Ag_45				-	-
PCL/PVA+Ag_60				-	-

Negative	Slowing growth	Positive	Not measured

Table 6: Antibacterial evaluation of prepared control fibrous samples and fibrous materials with Ag NPs against E. coli.

Sample	Incubation time				
	2 hours	3 hours	6 hours	12 hours	24 hours
	Growth inhibition (100 %)				
PCL fibres					
PCL/PVA_60					
PCL/PVA+Ag_15					
PCL/PVA+Ag_30					
PCL/PVA+Ag_45					
PCL/PVA+Ag_60				-	-

Negative	Slowing growth	Positive	Not measured

The prepared fibrous samples and their effect on cells require evaluation before being used as a clinical antibacterial. The PCL/PVA+Ag_60 sample, which showed the highest antibacterial activity for both tested bacteria cultures, was selected for cytotoxicity testing. Direct testing and MTT assay evaluated PCL, PCL/PVA_60 and PCL/PVA+Ag_60 samples herein.

Figure 30 shows that direct testing revealed little difference between these samples. While samples incubated for 24 hours had less vacuolisation than those incubated for 48 hours, and the 24 hours-incubation microscopy image had areas without cell

development compared to the 48 hours-incubation images, no changes in morphology or cell growth were observed after both these incubation periods. The ČSN EN ISO 10993-5 cytotoxicity guide to direct contact testing evaluated the samples as non-cytotoxic at stage zero. The life cycle of the cells in contact with this fibrous material was therefore not disturbed in any way. The tested surface had no effect on cell physical-chemical bonding and the cells could still replicate.

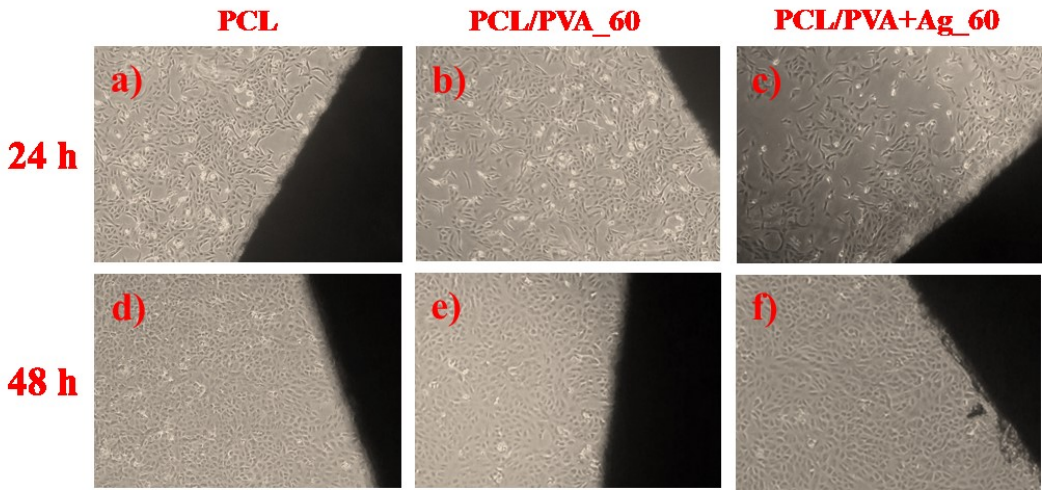

Figure 30: Microscope images of direct cytotoxicity testing after 24; control samples a) PCL fibres, b) PCL/PVA_60, c) PCL/PVA+Ag_60; and 48 hours; d) PCL fibres, e) PCL/PVA_60, f) PCL/PVA+Ag_60; magnification 50x.

The MTT assay is the most common method currently used in testing cell growth rate and culture medium toxicity. This is based on cell viability measurement, when yellow water-soluble MTT is reduce by the cells to blue-violet insoluble crystals of formazan to indicate cellular effect. The number of viable cells correlates with the colour intensity determined by photometric measurements after dissolving the formazan crystals in alcohol. Cytotoxic potential is then established if the sample viability is reduced to less than 70 % of the control [16, 25, 59].

Figure 31 shows the Vero cell suspension viability when PCL, PCL/PVA_60 and PCL/PVA+Ag_60 samples were tested by MTT assay. Cell viability was evaluated at decreasing 100, 50, 25 and 12.5 % extract concentrations. The PCL fibres established 91, 99, 106 and 106 % cell viability. The PCL/PVA sample had 90, 89, 92 and 92 % cell viability and the PCL/PVA+Ag_60 sample returned 82, 84, 86 and 89 %. These results determined that all samples were non-toxic to cells.

Control cell viability was also determined on decreasing extract concentration, and the PC viability values were 0, 1, 59 and 82 % and NC values were 97, 96, 98 and 99 %.

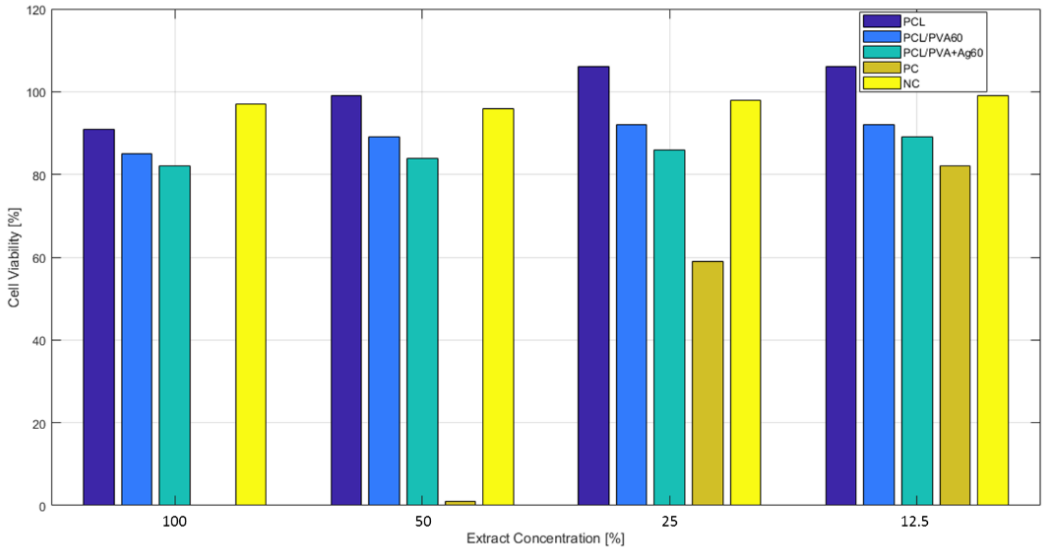

Figure 31: Viability of Vero cell suspension in the presence of samples; PCL fibres, PCL/PVA_60, PCL/PVA+Ag_60 and PC and NC control samples. Presence of samples in left to right colour order; PCL fibres, , PCL/PVA_60, PCL/PVA+Ag_60, PC and NC.

In conclusion, the material prepared in this thesis proved its potential for further modification and possible use in the biomedical field. This thesis material requires further investigation and the following changes may improve sample properties:

- construction of a multi-layered material where PCL fibres form the matrix and PVA droplets carriers the Ag NPs. This design would result in slower Ag NPs release than the material in this work, and also enhance the antibacterial effect.
- alteration of the morphology, size, surface properties or Ag NP agglomeration in this material.
- increasing PVA+Ag polymeric solution spraying time. This could also produce increased Ag NPs number droplets and greater antibacterial effect.

Conclusion

This diploma thesis was divided into two main parts – theoretical and experimental. The theoretical part contains a comprehensive literature review of the following three main topics: (1) an overview of the basic preparation methods of silver nanoparticles with detailed focus on phytosynthesis and its mechanism, (2) the encapsulation of the silver nanoparticles by electro-spraying and (3) the progressive materials used for polymer nanofibers and silver nanoparticles to enhance this antibacterial material's application in biomedical science.

The experimental part then focuses on the preparation and characterisation of the silver nanoparticles and the artificial material's subsequent effectiveness as an antibacterial agent. However, the 3-12 nanometre sized nanoparticles had low stability. Therefore, a possible mechanism for silver nanoparticles synthesis by metastable complexes was outlined, and this was primarily based on available information from both literature reviews and research analysis.

Both the prepared polymeric solutions of poly(vinyl alcohol) and the combined poly(vinyl alcohol) and silver nanoparticles were homogenous and successfully sprayed onto the poly(ε-caprolacton) fibrous matrix. Thus, the presence and incorporation of silver nanoparticles into poly(vinyl alcohol) droplets was proven.

In conclusion, the prepared fibrous materials transporting the silver nanoparticles exhibited antibacterial activity against *Staphylococcus aureus* and *Escherichia coli*. Moreover, the cytotoxicity testing established that the material with the most significant antibacterial activity was non-cytotoxic. Therefore, the interactions and experimental results presented herein strongly suggest that higher antibacterial activity can be achieved in the future and that this activity could led to higher cytotoxicity, as documented in this thesis.

References

[1] POOLE, Charles P. a Frank J. OWENS. *Introduction To Nanotechnology* [online]. 2003. ISBN 0471079359. Dostupné z: doi:10.1300/J105v21n01_01

[2] HORIKOSHI, Satoshi a Nick SERPONE. *Introduction to Nanoparticles* [online]. B.m.: Microwaves in Nanoparticle Synthesis: Fundamentals and Applications, 2013. ISBN 3527648127. Dostupné z: doi:10.1002/9783527648122.ch1

[3] STAMM, Manfred. Nanostructured and Nano-size Polymer Materials: How to generate them an DO We Need Them?. FAKIROV, Stoyko, ed. Nano-size Polymers [online]. Cham: Springer International Publishing, 2016. ISBN 9783319397153. Dostupné z: doi:10.1007/978-3-319-39715-3

[4] BINNIG, G. a H. ROHRER. Scanning tunneling microscopy. *IBM Journal of Research and Development*. 2000, **44**(1–2), 279–293. ISSN 00188646.

[5] VIEU, C., F. CARCENAC, A. PÉPIN, Y. CHEN, M. MEJIAS, A. LEBIB, L. MANIN-FERLAZZO, L. COURAUD a H. LAUNOIS. Electron beam lithography: Resolution limits and applications. *Applied Surface Science* [online]. 2000, **164**(1–4), 111–117. ISSN 01694332. Dostupné z: doi:10.1016/S0169-4332(00)00352-4

[6] FEYNMAN, Richard. *There's Plenty of Room at the Bottom: An Invitation to Enter a New Field of Physics*. 1959.

[7] PHU, Nguyen Dang, Luc Huy HOANG, Pham VAN HAI, Tran Quang HUY, Xiang Bai CHEN a Wu Ching CHOU. Photocatalytic activity enhancement of Bi2WO6 nanoparticles by Ag doping and Ag nanoparticles modification. *Journal of Alloys and Compounds* [online]. 2020, **824**, 153914. ISSN 09258388. Dostupné z: doi:10.1016/j.jallcom.2020.153914

[8] GHODAKE, Gajanan, Surendra SHINDE, Avinash KADAM, Rijuta Ganesh SARATALE, Ganesh Dattatraya SARATALE, Asad SYED, Omar SHAIR, Marzouq ALSAEDI a Dae Young KIM. Gallic acid-functionalized silver nanoparticles as colorimetric and spectrophotometric probe for detection of Al^{3+} in aqueous medium. *Journal of Industrial and Engineering Chemistry* [online]. 2020, **82**, 243–253. ISSN 22345957. Dostupné z: doi:10.1016/j.jiec.2019.10.019

[9] HUSSIN, Farihahusnah a Mohamed Kheireddine AROUA. Recent trends in the development of adsorption technologies for carbon dioxide capture: A brief literature and patent reviews (2014–2018). *Journal of Cleaner Production* [online]. 2020, **253**,

119707. ISSN 09596526. Dostupné z: doi:10.1016/j.jclepro.2019.119707

[10] MIKES, Petr, Jana HORAKOVA, Ales SAMAN, Lucie VEJSADOVA, Paul TOPHAM, Winita PUNYODOM, Manita DUMKLANG a Vera JENCOVA. Comparison and characterization of different polyester nano/micro fibres for use in tissue engineering applications. *Journal of Industrial Textiles* [online]. 2019. ISSN 15308057. Dostupné z: doi:10.1177/1528083719848155

[11] MOHSENI, Mina, Amir SHAMLOO, Zahra AGHABABAIE, Homa AFJOUL a Shabnam ABDI. A comparative study of wound dressings loaded with silver sulfadiazine and silver nanoparticles: In vitro and in vivo evaluation. *International Journal of Pharmaceutics* [online]. 2019, **564**(April), 350–358. ISSN 0378-5173. Dostupné z: doi:10.1016/j.ijpharm.2019.04.068

[12] KRATOŠOVÁ, Gabriela, Veronika HOLIŠOVÁ, Zuzana KONVIČKOVÁ, Avinash P. INGLE, Swapnil GAIKWAD, Kateřina ŠKRLOVÁ, Aleš PROKOP, Mahendra RAI a Daniela PLACHÁ. From biotechnology principles to functional and low-cost metallic bionanocatalysts. *Biotechnology Advances* [online]. 2019, **37**(1), 154–176. ISSN 07349750. Dostupné z: doi:10.1016/j.biotechadv.2018.11.012

[13] ALAVI, Mehran a Naser KARIMI. Biosynthesis of Ag and Cu NPs by secondary metabolites of usnic acid and thymol with biological macromolecules aggregation and antibacterial activities against multi drug resistant (MDR) bacteria. *International Journal of Biological Macromolecules* [online]. 2019, **128**, 893–901. ISSN 18790003. Dostupné z: doi:10.1016/j.ijbiomac.2019.01.177

[14] KUZOVNIKOVA, Ludmila, Sergey KOMOGORTSEV, Elena DENISOVA, Rauf ISKHAKOV, Ivan NEMTSEV, Mikhail VOLOCHAEV a Natalia SHEPETA. Structure and magnetism in ball-milled core-shell Al2O3@Co particles. *Materials Today: Proceedings* [online]. 2019, **12**, 159–162. ISSN 22147853. Dostupné z: doi:10.1016/j.matpr.2019.03.087

[15] LÉON, Aline, Oleg ZABARA, Sabrina SARTORI, Nico EIGEN, Martin DORNHEIM, Thomas KLASSEN, Jiri MULLER, Bjørn HAUBACK a Maximilian FICHTNER. Investigation of (Mg, Al, Li, H)-based hydride and alanate mixtures produced by reactive ball milling. *Journal of Alloys and Compounds* [online]. 2009, **476**(1–2), 425–428. ISSN 09258388. Dostupné z: doi:10.1016/j.jallcom.2008.09.023

[16] SAHU, Nidhi, Deepika SONI, B. CHANDRASHEKHAR, D. B. SATPUTE, Sivanesan SARAVANADEVI, B. K. SARANGI a R. A. PANDEY. Synthesis of silver

nanoparticles using flavonoids: hesperidin, naringin and diosmin, and their antibacterial effects and cytotoxicity. *International Nano Letters* [online]. 2016, **6**(3), 173–181. ISSN 2008-9295. Dostupné z: doi:10.1007/s40089-016-0184-9

[17] VILAMOVÁ, Zuzana, Zuzana KONVIČKOVÁ, Petr MIKEŠ, Veronika HOLIŠOVÁ, Pavel MANČÍK, Edmund DOBROČKA, Gabriela KRATOŠOVÁ a Jana SEIDLEROVÁ. Ag-AgCl Nanoparticles Fixation on Electrospun PVA Fibres: Technological Concept and Progress. *Scientific Reports* [online]. 2019, **9**, 1–10. Dostupné z: doi:10.1038/s41598-019-51642-7

[18] SPAGNOLETTI, Federico N., Cecilia SPEDALIERI, Florencia KRONBERG a Romina GIACOMETTI. Extracellular biosynthesis of bactericidal Ag/AgCl nanoparticles for crop protection using the fungus Macrophomina phaseolina. *Journal of Environmental Management* [online]. 2019, **231**, 457–466. ISSN 10958630. Dostupné z: doi:10.1016/j.jenvman.2018.10.081

[19] GU, Haidong, Xiao CHEN, Feng CHEN, Xing ZHOU a Zohreh PARSAEE. Ultrasound-assisted biosynthesis of CuO-NPs using brown alga Cystoseira trinodis: Characterization, photocatalytic AOP, DPPH scavenging and antibacterial investigations. *Ultrasonics Sonochemistry* [online]. 2018, **41**(July 2017), 109–119. ISSN 18732828. Dostupné z: doi:10.1016/j.ultsonch.2017.09.006

[20] GAŁUSZKA, Agnieszka, Zdzisław MIGASZEWSKI a Jacek NAMIEŚNIK. The 12 principles of green analytical chemistry and the SIGNIFICANCE mnemonic of green analytical practices. *Trends in Analytical Chemistry* [online]. 2013, **50**, 78–84. ISSN 18793142. Dostupné z: doi:10.1016/j.trac.2013.04.010

[21] KHAN, Ibrahim, Khalid SAEED a Idrees KHAN. Nanoparticles: Properties, applications and toxicities. *Arabian Journal of Chemistry* [online]. 2019, **12**(7), 908–931. ISSN 18785352. Dostupné z: doi:10.1016/j.arabjc.2017.05.011

[22] ALAVI, Mehran a Naser KARIMI. Characterization, antibacterial, total antioxidant, scavenging, reducing power and ion chelating activities of green synthesized silver, copper and titanium dioxide nanoparticles using Artemisia haussknechtii leaf extract. *Artificial Cells, Nanomedicine and Biotechnology* [online]. 2018, **46**(8), 2066–2081. ISSN 2169141X. Dostupné z: doi:10.1080/21691401.2017.1408121

[23] HAES, AJ a RP Van DUYNE. A Nanoscale Optical Biosensor: Sensitivity and Selectivity of an Approach Based on the Localized Surface Plasmon Resonance Spectroscopy of Triangular Silver Nanoparticles. *J. Am. Chem. Soc* [online]. 2002, (7),

10596–10604. Dostupné z: http://pubs.acs.org/cgi-bin/cen/trustedproxy.cgi?redirect=http://pubs.acs.org/doi/abs/10.1021/ja020393x

[24] LEE, Sang Hun a Bong Hyun JUN. Silver nanoparticles: Synthesis and application for nanomedicine. *International Journal of Molecular Sciences* [online]. 2019, **20**(4). ISSN 14220067. Dostupné z: doi:10.3390/ijms20040865

[25] LI, Dan, Zuojia LIU, Ye YUAN, Yawen LIU a Fenglan NIU. Green synthesis of gallic acid-coated silver nanoparticles with high antimicrobial activity and low cytotoxicity to normal cells. *Process Biochemistry* [online]. 2015, **50**(3), 357–366. ISSN 13595113. Dostupné z: doi:10.1016/j.procbio.2015.01.002

[26] KHAN, Mujeeb, Mohammed Rafi SHAIK, Syed Farooq ADIL, Shams Tabrez KHAN, Abdulrahman AL-WARTHAN, Mohammed Rafiq H. SIDDIQUI, Muhammad N. TAHIR a Wolfgang TREMEL. Plant extracts as green reductants for the synthesis of silver nanoparticles: lessons from chemical synthesis. *Dalton Transactions* [online]. 2018, **47**(35), 11988–12010. ISSN 14779234. Dostupné z: doi:10.1039/C8DT01152D

[27] DUNNE, Peter W., Alexis S. MUNN, Chris L. STARKEY, Tom A. HUDDLE a Ed H. LESTER. Continuous-flow hydrothermal synthesis for the production of inorganic nanomaterials. *Philosophical Transactions of the Royal Society A: Mathematical, Physical and Engineering Sciences* [online]. 2015, **373**(2057). ISSN 1364503X. Dostupné z: doi:10.1098/rsta.2015.0015

[28] FERESHTEH, Zeinab, Ramin ROJAEE a Ali SHARIFNABI. Effect of different polymers on morphology and particle size of silver nanoparticles synthesized by modifid polyol method. *Superlattices and Microstructures* [online]. 2016, **98**, 267–275. ISSN 0749-6036. Dostupné z: doi:10.1016/j.spmi.2016.08.034

[29] AGUIRRE-HERNÁNDEZ, Eva, Ma Eva GONZÁLEZ-TRUJANO, Ana Laura MARTÍNEZ, Julia MORENO, Geoffrey KITE, Teresa TERRAZAS a Marcos SOTO-HERNÁNDEZ. HPLC/MS analysis and anxiolytic-like effect of quercetin and kaempferol flavonoids from Tilia americana var. mexicana. *Journal of Ethnopharmacology* [online]. 2010, **127**(1), 91–97. ISSN 03788741. Dostupné z: doi:10.1016/j.jep.2009.09.044

[30] ONISZCZUK, Anna a Rafał PODGÓRSKI. Influence of different extraction methods on the quantification of selected flavonoids and phenolic acids from Tilia cordata inflorescence. *Industrial Crops and Products* [online]. 2015, **76**, 509–514. ISSN 09266690. Dostupné z: doi:10.1016/j.indcrop.2015.07.003

[31] JAIN, Siddhant a Mohan Singh MEHATA. Medicinal Plant Leaf Extract and Pure Flavonoid Mediated Green Synthesis of Silver Nanoparticles and their Enhanced Antibacterial Property. *Scientific Reports* [online]. 2017, (November), 1–13. ISSN 2045-2322. Dostupné z: doi:10.1038/s41598-017-15724-8

[32] ALAVI, Mehran, Naser KARIMI a Tahereh VALADBEIGI. Antibacterial, Antibiofilm, Antiquorum Sensing, Antimotility, and Antioxidant Activities of Green Fabricated Ag, Cu, TiO2, ZnO, and Fe3O4 NPs via Protoparmeliopsis muralis Lichen Aqueous Extract against Multi-Drug-Resistant Bacteria. *ACS Biomaterials Science and Engineering* [online]. 2019, **5**(9), 4228–4243. ISSN 23739878. Dostupné z: doi:10.1021/acsbiomaterials.9b00274

[33] KIM, Dae Young, Jung SUK SUNG, Min KIM a Gajanan GHODAKE. Rapid production of silver nanoparticles at large-scale using gallic acid and their antibacterial assessment. *Materials Letters* [online]. 2015, **155**, 62–64. ISSN 18734979. Dostupné z: doi:10.1016/j.matlet.2015.04.138

[34] MORTON, W. J. Method of Dispersing Fluids. 705 691. 1902. United states.

[35] ZELENY, John. The Electrical Discharge from Liquid Points, and a Hydrostatic Method of Measuring the Electric Intensity at Their Surfaces. *Phys. Rev 3*. 1914, **3**(2).

[36] LUKÁŠ, D., A. SARKAR, L. MARTINOVÁ, K. VODSED'ÁLKOVÁ, D. LUBASOVÁ, J. CHALOUPEK, P. POKORNÝ, P. MIKEŠ, J. CHVOJKA a M. KOMÁREK. Physical principles of electrospinning (electrospinning as a nano-scale technology of the twenty-first century). *Textile Progress* [online]. 2009, **41**(2), 59–140. ISSN 00405167. Dostupné z: doi:10.1080/00405160902904641

[37] JIRSAK, Oldrich, Filip SANETRNIK, Vaclav KOTEK, Lenka MARTINOVA a Jiri CHALOUPEK. METHOD OF NANOFIBRES PRODUCTION FROMIA POLYMER SOLUTION USING ELECTROSTATC SPINNING AND A DEVICE FOR CARRYING OUT THE METHOD. US 7,585,437 B2. 2006. Czech Republic.

[38] WANG, Min a Qilong ZHAO. Electrospinning and Electrospray for Biomedical Applications. *Encyclopedia of Biomedical Engineering* [online]. 2018, 1–15. Dostupné z: doi:10.1016/B978-0-12-801238-3.11028-1

[39] NGUYEN, Duong Nhat, Christian CLASEN a Guy VAN DEN MOOTER. Pharmaceutical Applications of Electrospraying. *Journal of Pharmaceutical Sciences* [online]. 2016, **105**(9), 2601–2620. ISSN 15206017. Dostupné z: doi:10.1016/j.xphs.2016.04.024

[40] REPANAS, Alexandros a Birgit GLASMACHER. The signifcance of electrospinning as a method to create fibrous scaffolds for biomedical engineering and drug delivery applications [online]. 2016, **31**. Dostupné z: doi:10.1016/j.jddst.2015.12.007

[41] WANG, Min a Hong KONG. *Electrospinning and Electrospray for Biomedical Applications* [online]. B.m.: Elsevier Inc., 2018. ISBN 9780128012383. Dostupné z: doi:10.1016/B978-0-12-801238-3.11028-1

[42] TSIAPLA, A R, V BAKOLA, V KARAGKIOZAKI, E PAVLIDOU a S LOGOTHETIDIS. Biodegradable Electrosprayed NPs as Drug Carriers for Optimal Treatment of Orthopaedic Infections. *Materials Today: Proceedings* [online]. 2019, **19**, 110–116. ISSN 2214-7853. Dostupné z: doi:10.1016/j.matpr.2019.07.665

[43] BODA, Sunil Kumar, Xiaoran LI a Jingwei XIE. Electrospraying an enabling technology for pharmaceutical and biomedical applications: A review. *Journal of Aerosol Science* [online]. 2018, **125**, 164–181. ISSN 18791964. Dostupné z: doi:10.1016/j.jaerosci.2018.04.002

[44] HASSIBA, Alaa J., Mohamed E. EL ZOWALATY, Thomas J. WEBSTER, Aboubakr M. ABDULLAH, Gheyath K. NASRALLAH, Khalil Abdelrazek KHALIL, Adriaan S. LUYT a Ahmed A. ELZATAHRY. Synthesis, characterization, and antimicrobial properties of novel double layer nanocomposite electrospun fibers for wound dressing applications. *International Journal of Nanomedicine* [online]. 2017, **12**, 2205–2213. ISSN 11782013. Dostupné z: doi:10.2147/IJN.S123417

[45] MOHSENI, Mina, Amir SHAMLOO, Zahra AGHABABAIE, Homa AFJOUL, Shabnam ABDI, Hamideh MORAVVEJ a Manouchehr VOSSOUGHI. A comparative study of wound dressings loaded with silver sulfadiazine and silver nanoparticles: In vitro and in vivo evaluation. *International Journal of Pharmaceutics* [online]. 2019, **564**(November 2018), 350–358. ISSN 18733476. Dostupné z: doi:10.1016/j.ijpharm.2019.04.068

[46] KHOSHNOUDI-NIA, Sara, Niloufar SHARIF a Seid MAHDI. Loading of phenolic compounds into electrospun nanofibers and electrosprayed nanoparticles. *Trends in Food Science & Technology* [online]. 2020, **95**(November 2019), 59–74. ISSN 0924-2244. Dostupné z: doi:10.1016/j.tifs.2019.11.013

[47] ZAMANI, Maedeh, Molamma P PRABHAKARAN a Eng SAN. Protein encapsulated core–shell structured particles prepared by coaxial electrospraying: Investigation on material and processing variables. *International Journal of Pharmaceutics* [online].

2014, **473**(1–2), 134–143. ISSN 0378-5173. Dostupné z: doi:10.1016/j.ijpharm.2014.07.006

[48] OGUR, E. *Polyvinyl alcohol: materials, processing and applications*. 2005. ISBN 978-1-84735-095-4.

[49] VAN NATTA, Frank J., Julian W. HILL a Wallace H. CAROTHERS. Studies of Polymerization and Ring Formation. XXIII. Caprolactone and its Polymers. *J. Am. Chem. Soc.* 1934, **56**(5), 455–459.

[50] GUARINO, Vincenzo, Gennaro GENTILE, Luigi SORRENTINO a Luigi AMBROSIO. *Polycaprolactone: synthesis, properties, and applications* [online]. Encycloped. B.m.: John Wiley & Sons, Inc, 2017. ISBN 0471440264. Dostupné z: doi:10.1002/0471440264.pst658

[51] AZIMI, Bahareh, Parviz NOURPANAH, Mohammad RABIEE a Shahram ARBAB. Poly (ε-caprolactone) Fiber: An Overview. *Journal of Engineered Fibers and Fabrics* [online]. 2014, **9**(3), 74–90. Dostupné z: https://www.jeffjournal.org/papers/Volume9/V9I3 (9) P. Nourpanah.pdf

[52] ZHANG, Y. Z., J. VENUGOPAL, Z. M. HUANG, C. T. LIM a S. RAMAKRISHNA. Characterization of the surface biocompatibility of the electrospun PCL-Collagen nanofibers using fibroblasts. *Biomacromolecules* [online]. 2005, **6**(5), 2583–2589. ISSN 15257797. Dostupné z: doi:10.1021/bm050314k

[53] LIU, Zhufeng, Anyi ZHOU, Xiaojin ZHANG a Cailing ZHAO. The efficacy of nano-silver and silver sulfadiazine for degree II burn wound: a meta-analysis. *Biomedical Research* [online]. 2017, **28**(9), 3880–3885. Dostupné z: https://www.alliedacademies.org/articles/the-efficacy-of-nanosilver-and-silver-sulfadiazine-for-degree-ii-burn-wound-a-metaanalysis.html

[54] QIAN, Li-Wu, Andrea B. FOURCAUDOT a Kai P. LEUNG. Cite Permissions Icon Permissions Share Article Navigation Silver Sulfadiazine Retards Wound Healing and Increases Hypertrophic Scarring in a Rabbit Ear Excisional Wound Model. *Journal of Burn Care & Research* [online]. 2017, **38**(1), 418–422. Dostupné z: https://academic.oup.com/jbcr/article-abstract/38/1/e418/4568957?redirectedFrom=fulltext

[55] SMITH, G., D. S. SAGATYS, C. DAHLGREN, D. E. LYNCH, R. C. BOTT, K. A. BYRIEL a C. H.L. KENNARD. Structures of the silver (I) complexes with maleic and fumaric acids: Silver(I) hydrogen maleate, silver(I) maleate and silver (I) fumarate.

Zeitschrift fur Kristallographie - New Crystal Structures [online]. 1995, **210**(1), 44–48. ISSN 00442968. Dostupné z: doi:10.1524/zkri.1995.210.1.44

[56] Silver Colloids [online]. nedatováno. Dostupné z: http://www.silver-colloids.com/Tutorials/Intro/pcs18A.html

[57] CHOU, H. L., C. M. WU, F. D. LIN a J. RICK. Interactions between silver nanoparticles and polyvinyl alcohol nanofibers. *AIP Advances* [online]. 2014, **4**(8). ISSN 21583226. Dostupné z: doi:10.1063/1.4890290

[58] PIRTARIGHAT, Saba, Maryam GHANNADNIA a Saeid BAGHSHAHI. Biosynthesis of silver nanoparticles using Ocimum basilicum cultured under controlled conditions for bactericidal application. *Materials Science & Engineering C* [online]. 2019, **98**(July 2018), 250–255. ISSN 0928-4931. Dostupné z: doi:10.1016/j.msec.2018.12.090

[59] LI, WEIJIA, JING ZHOU a YUYIN XU. Study of the in vitro cytotoxicity testing of medical devices (Review). *Biomedical Reports* [online]. 2015, **3**(5), 617–620. ISSN 2049-9434. Dostupné z: doi:10.3892/br.2015.481